J. Fluid Mech. (1981), *vol.* 111, *pp.* 141–173
Printed in Great Britain

Heat transfer in a layered porous medium heated from below

By R. McKIBBIN AND M. J. O'SULLIVAN
Department of Theoretical and Applied Mechanics, University of Auckland, New Zealand

(Received 21 July 1980 and in revised form 13 February 1981)

Previous work by the present authors on the onset of convection in a layered porous medium heated from below is extended to an investigation of the heat transported by convection at slightly supercritical Rayleigh numbers.

The two-dimensional convection patterns and associated values of the critical Rayleigh number, cell width and slope of the Nusselt-number graph are calculated for two- and three-layer configurations over a wide range of layer depth and permeability ratios. The results show that the commonly studied problem of a homogeneous layer bounded above and below by impermeable boundaries is a special case, in that the slope of the Nusselt-number graph at the critical point is nearly independent of cell width. For a homogeneous layer with a permeable upper boundary, and for multi-layered systems, the slope of this graph depends strongly on cell width.

1. Introduction

The amount of heat that is transported by convection through a fluid-saturated porous medium is of considerable interest because of its association with the modelling of geothermal fields. The earliest work, including that of Lapwood (1948), established that convection can occur in a horizontal layer between isothermal boundaries for Rayleigh numbers above a certain value. Subsequent research has been directed at more complicated onset problems, and finite-amplitude motion at supercritical Rayleigh numbers for homogeneous layers and, in a small number of cases, for more complicated configurations. A summary of this work is provided in an excellent review by Cheng (1978).

Associated with the numerous works on finite-amplitude convection in a homogeneous layer (see, for example, Elder 1967; Straus 1974; Caltagirone 1975; Joseph 1976; Horne & O'Sullivan 1978*a*, *b*; Schubert & Straus 1979) have been estimates of the heat flux produced by such convection. An analytical approximation for the Nusselt number, which measures the heat flow, was found by Palm, Weber & Kvernvold (1972) for a homogeneous layer using a perturbation technique. The resulting sixth-order expression was found to agree reasonably well, at Rayleigh numbers several times the critical value, with the many numerical results derived by the above authors and with experimental results.

Recently, three studies of convection in a more general inhomogeneous layer have been made. Masuoka *et al.* (1978) examined the criterion for onset of convection in a porous medium composed of two layers of different permeabilities or thermal conductivities. They found that increasing non-homogeneities in permeability or conductivity led to transitions of flow patterns from 'large-scale' convection occurring throughout both layers to 'local' convection confined mainly to one of the two

layers. Rana, Horne & Cheng (1979) numerically investigated finite-amplitude convection in a three-layer model of the Pahoa reservoir in Hawaii. The criterion for onset of convection in a porous medium comprising an arbitrary number of separately homogeneous layers of different depths, permeabilities and conductivities was established by McKibbin & O'Sullivan (1980). They also noted the transition of flow patterns similar to those found by Masuoka *et al.* (1978).

The present paper extends the previous work of the present authors on the onset problem to an examination of post-onset behaviour and provides estimates of the heat transported by convection in a general layered system for slightly supercritical Rayleigh numbers. Since, in a geothermal context, inhomogeneity, particularly layering, is common, the problem has much practical importance. In particular it is of interest to use observations of surface or near-surface heat flux to deduce the depth of the geothermal heat source and the permeability structure of the system.

The analysis presented can be applied to any number of layers and provides the criterion for onset, the cell-width and convection pattern, and the slope of the graph of the Nusselt number for slightly supercritical Rayleigh numbers. Because of the wide variety of possible configurations and values of various parameters, detailed results are presented only for the two- and three-layer cases. These represent idealized model geothermal fields where a permeable zone either overlies or is overlain by a less permeable layer, or where a horizontal aquifer occurs in the interior of a matrix with a different permeability.

For the configurations considered the variation of heat transfer with cell width is investigated. One of the most interesting results obtained is that the onset mode (either a single wide two-dimensional roll or many narrow two-dimensional rolls at the critical Rayleigh number) does not necessarily maximize the heat transferred at Rayleigh numbers above critical. Also it is found that, for all cases studied, except the uniform layer with a closed top, the heat transfer is strongly dependent on cell-width and is maximum, for supercritical Rayleigh numbers, at a cell-width different from that for onset.

2. Problem formulation

A saturated permeable layer of total thickness d, comprising N separate homogeneous layers, is considered. The thickness, permeability and thermal conductivity may vary from layer to layer. The system is bounded below (beneath layer 1) by an impermeable isothermal surface, at a temperature $T_a+\Delta T$. Here, T_a is the (atmospheric) temperature of the top surface, which is considered to be either impermeable (case A) or at constant (atmospheric) pressure p_a (case B). (See figure 1.)

Within a typical stratum, layer i, of thickness d_i, the usual equations of conservation of mass and energy, and Darcy's law are assumed to hold:

$$m_i \frac{\partial \rho}{\partial t} + \nabla . \mathbf{v} = 0, \tag{1}$$

$$\frac{\partial}{\partial t}[m_i \rho c T + (1-m_i)\rho_i c_i T] + \nabla . (cT\mathbf{v}) = k_i \nabla^2 T, \tag{2}$$

$$\nabla p = \rho \mathbf{g} - \frac{\nu}{K_i}\mathbf{v}. \tag{3}$$

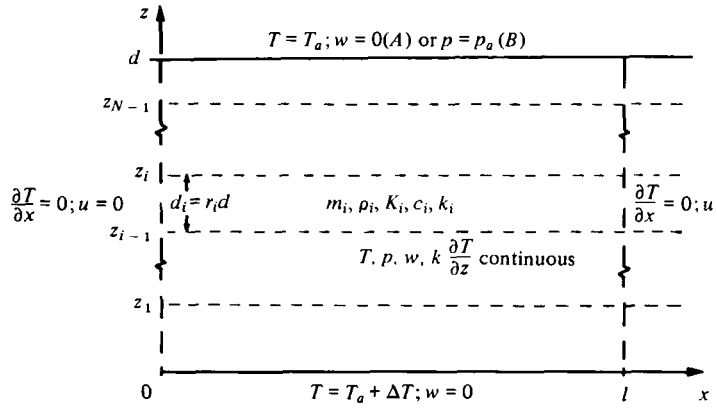

FIGURE 1. Schematic diagram of configuration considered – a porous medium comprising N homogeneous horizontal layers.

Here m_i, K_i, ρ_i, c_i are respectively the porosity, permeability, density and specific heat of the porous matrix in layer i, k_i is the thermal conductivity of the saturated medium, ρ, c, ν, $\mathbf{v}$ are respectively the density, specific heat, kinematic viscosity and mass flux vector of the fluid and T and p are the temperature and pressure at a point within the saturated porous medium. The acceleration due to gravity is represented by the vector $\mathbf{g}$.

The density of the saturating fluid is assumed to vary linearly with temperature,

$$\rho = \rho_a[1-\alpha(T-T_a)],$$

where α is a constant and ρ_a is the density of the fluid at temperature T_a.

For small (but finite) amplitude convection in the system, only steady solutions are of interest. The stability of steady two-dimensional convection in a homogeneous layer has been investigated by Straus (1974). He established that, provided the Rayleigh number R is small enough, there is a range of horizontal wavenumbers over which the basic roll convection pattern is stable. In a paper by Straus & Schubert (1978) further investigation of the stability of such a flow when confined within a rectangular box revealed that, for small enough values of R, it was unlikely that there were box dimensions for which a stable steady two-dimensional flow could not occur. In a later paper by the same authors (1979), they noted that their results showed that it was always possible to force either steady two-dimensional or steady three-dimensional convection by proper choice of initial conditions. It thus seems reasonable, in the layered systems being investigated in this paper, to assume that two-dimensional flows can exist for slightly supercritical conditions, whether the system is confined in a rectangular box or not; therefore in the following analysis only the two-dimensional region $0 < x < l$, $0 < z < d$ is considered. On the lateral boundaries, corresponding to the limits of each convection cell or possibly to some physical boundary, conditions of no horizontal fluid flow or heat flow are imposed. Taking $\mathbf{v} = (u, 0, w)$ and assuming all variables depend only on x and z, (1)–(3), for layer i, become:

$$\frac{\partial u}{\partial x} + \frac{\partial w}{\partial z} = 0, \tag{4}$$

$$c\left(u\frac{\partial T}{\partial x}+w\frac{\partial T}{\partial z}\right)=k_i\left(\frac{\partial^2 T}{\partial x^2}+\frac{\partial^2 T}{\partial z^2}\right), \tag{5}$$

$$\frac{\partial p}{\partial x}=-\frac{\nu}{K_i}u, \tag{6}$$

$$\frac{\partial p}{\partial z}=-\rho_a[1-\alpha(T-T_a)]\,g-\frac{\nu}{K_i}w, \tag{7}$$

for $0<x<l$, $z_{i-1}<z<z_i$, where $z_i=\Sigma_{j=1}^{i}d_j$. (For steady flows, the use of mass flows as variables avoids the need to use the Boussinesq approximation.)

The thermal and fluid boundary conditions at the bottom and top of the system are, respectively:

$$T=T_a+\Delta T \quad \text{and} \quad w=0 \quad \text{on} \quad z=0,$$

$$T=T_a \quad \text{and} \quad \left\{\begin{matrix} w=0 & \text{(case A)} \\ p=p_a & \text{(case B)}\end{matrix}\right\} \quad \text{on} \quad z=d.$$

Continuity in temperature, pressure, vertical mass flux and vertical heat flux requires T, p, w and $cTw-k\,\partial T/\partial z$ to be continuous at each interface. Using the continuity of T and w, the last condition is simplified to the continuity of $k\,\partial T/\partial z$ at each interface.

The flow of heat through the system may be measured by considering Nu^*, the mean vertical heat flux over one cell, defined by

$$Nu^*=\frac{1}{l}\int_0^l\left(cTw-k\frac{\partial T}{\partial z}\right)_{z=h}dx,$$

where the measurement is made at height h, $0\leqslant h\leqslant d$. It is easily shown, by integrating (5) with respect to x, that Nu^* does not vary with z. Therefore the value at the base of the system (where $w=0$) can be used,

$$Nu^*=\frac{1}{l}\int_0^l\left(-k_1\frac{\partial T}{\partial z}\right)_{z=0}dx. \tag{8}$$

The basic procedure, to determine the solution to (4)–(7) and hence evaluate Nu^*, is to investigate small (but finite) perturbations to the conduction solution ($u=w=0$). The conduction solution for the temperature T_c is a piecewise linear function given by

$$T_c=T_a+\Delta T\left(\sum_{j=i}^{N}\delta_j-\frac{z-z_{i-1}}{k_i}\right)\Big/\delta$$

for $z_{i-1}<z<z_i$, where $\delta_i=d_i/k_i$ and $\delta=\Sigma_{j=1}^{N}\delta_j$. This distribution corresponds to a temperature drop ΔT_i across layer i given by

$$\Delta T_i=\frac{\delta_i}{\delta}\Delta T.$$

Following the standard perturbation procedure, we substitute $u=u'$, $w=w'$, $T=T_c+T'$, $p=p_c+p'$ [p_c is obtained from T_c by using (7) and the requirement that p_c be continuous at each interface]. It is convenient to non-dimensionalize the variables differently in each layer; for layer i the variables are defined by

$$T_i=T'/\Delta T_i, \quad p_i=p'K_ic/\nu r_ik_i,$$
$$(u_i,w_i)=(u',w')\,cd/r_ik_i, \quad X=x/d,$$
$$Z_i=(z-z_{i-1})/d_i.$$

Here $r_i = d_i/d$ is the fraction of the total layer thickness occupied by layer i. Substitution into (4)–(7) of these non-dimensional perturbations to the conduction solution gives, for layer i,

$$\frac{\partial u_i}{\partial X} + \frac{1}{r_i}\frac{\partial w_i}{\partial Z_i} = 0, \tag{9}$$

$$r_i u_i \frac{\partial T_i}{\partial X} + w_i\left(\frac{\partial T_i}{\partial Z_i} - 1\right) = \frac{\partial^2 T_i}{\partial X^2} + \frac{1}{r_i^2}\frac{\partial^2 T_i}{\partial Z_i^2}, \tag{10}$$

$$\frac{\partial p_i}{\partial X} = -u_i, \tag{11}$$

$$\frac{1}{r_i}\frac{\partial p_i}{\partial Z_i} = \frac{R_i}{r_i^2} T_i - w_i. \tag{12}$$

for $0 < X < L$, $0 < Z_i < 1$ and $i = 1, 2, \ldots, N$, where $L = l/d$ is the non-dimensionalized cell width. The Rayleigh number R_i for layer i, given by

$$R_i = \frac{\rho_a g K_i c \alpha \Delta T_i d_i}{\nu k_i},$$

is based on the layer depth d_i and the layer temperature drop ΔT_i.

For later reference, we also define a parameter R, given by

$$R = \frac{\delta d}{\delta_1 d_1}\frac{R_1}{4\pi^2} = \frac{\rho_a g K_1 c \alpha \Delta T d}{4\pi^2 \nu k_1}.$$

This parameter R is a Rayleigh number, given in terms of the thickness and temperature drop of the whole system and the conductivity and permeability of layer 1, divided by $4\pi^2$, which is the *minimum* critical value for a homogeneous layer with an impermeable top. The relationship between R_1 and R is clear from the above. The Rayleigh number for each layer R_i can also be related to R_1 and then to R using the relationship

$$\frac{R_i}{R_1} = \frac{K_i d_i^2}{k_i^2}\frac{k_1^2}{K_1 d_1^2}.$$

The heat transferred by the conduction solution is

$$\begin{aligned} Nu_c^* &= \frac{1}{l}\int_0^l -k_1\left(\frac{\partial T_c}{\partial z}\right)_{z=0} dx \\ &= \Delta T/\delta. \end{aligned}$$

We now introduce the standard Nusselt number Nu, defined as the ratio of the heat transferred by convection and conduction to that transferred by conduction alone, and given by

$$\begin{aligned} Nu &= Nu^*/Nu_c^* \\ &= \frac{1}{L}\int_0^L \left(1 - \frac{\partial T_1}{\partial Z_1}\right)_{Z_1=0} dX \end{aligned} \tag{13}$$

when expressed in terms of the non-dimensionalized variables.

To aid the solution of (9)–(12) a stream function ψ_i for layer i is introduced so that

$$u_i = \frac{1}{r_i}\frac{\partial \psi_i}{\partial Z_i}, \quad w_i = -\frac{\partial \psi_i}{\partial X}$$

to satisfy the equation of conservation of mass (9). Substitution into (10)–(12), and elimination of p_i gives a pair of equations for T_i and ψ_i:

$$\frac{\partial^2\psi_i}{\partial X^2}+\frac{1}{r_i^2}\frac{\partial^2\psi_i}{\partial Z_i^2}=-\frac{R_i}{r_i^2}\frac{\partial T_i}{\partial X}, \tag{14}$$

$$\frac{\partial^2 T_i}{\partial X^2}+\frac{1}{r_i^2}\frac{\partial^2 T_i}{\partial Z_i^2}=\frac{\partial\psi_i}{\partial X}+\frac{\partial\psi_i}{\partial Z_i}\frac{\partial T_i}{\partial X}-\frac{\partial\psi_i}{\partial X}\frac{\partial T_i}{\partial Z_i}, \tag{15}$$

for $0 < X < L$, $0 < Z_i < 1$ and $i = 1, 2, \ldots, N$. The boundary conditions can be expressed in terms of the non-dimensional quantities T_i, ψ_i as follows: On $Z_1 = 0$,

$$T_1 = 0 \quad \text{and} \quad \psi_1 = 0. \tag{16a}$$

On $Z_i = 1$ or $Z_{i+1} = 0$,

$$\left.\begin{aligned} \frac{r_i}{k_i}T_i=\frac{r_{i+1}}{k_{i+1}}T_{i+1}, \quad r_i k_i\psi_i = r_{i+1}k_{i+1}\psi_{i+1}, \\ \frac{\partial T_i}{\partial Z_i}=\frac{\partial T_{i+1}}{\partial Z_{i+1}}, \quad \frac{k_i}{K_i}\frac{\partial\psi_i}{\partial Z_i}=\frac{k_{i+1}}{K_{i+1}}\frac{\partial\psi_{i+1}}{\partial Z_{i+1}} \end{aligned}\right\} \tag{16b}$$

for $i = 1, 2, \ldots, N-1$. On $Z_N = 1$,

$$T_N = 0 \quad \text{and} \quad \psi_N = 0 \quad \text{(case A)} \quad \text{or} \quad \frac{\partial\psi_N}{\partial Z_N} = 0 \quad \text{(case B)}. \tag{16c}$$

On the lateral boundaries $X = 0$ and $X = L$,

$$\frac{\partial T_i}{\partial X} = 0 \quad \text{and} \quad \psi_i = 0. \tag{16d}$$

3. The perturbation procedure

For a given physical configuration there is a minimum temperature difference ΔT_c across the system which can produce the onset of two-dimensional convection with a cell-width L. The value ΔT_c corresponds to the minimum critical Rayleigh number for the system, $R = R_c$ (see McKibbin & O'Sullivan 1980). For values of ΔT above ΔT_c ($R > R_c$) a finite-amplitude flow can exist. Following Palm *et al.* (1972), we define a parameter ϵ, where

$$\begin{aligned} \epsilon^2 &= (\Delta T - \Delta T_c)/\Delta T \\ &= (R - R_c)/R = (R_i - R_{ic})/R_i, \end{aligned} \tag{17}$$

where R_{ic} is the critical value of the layer Rayleigh number R_i, $i = 1, 2, \ldots, N$. The value of ϵ remains less than unity for all values of $\Delta T > \Delta T_c$. The solutions T_i, ψ_i of (14), (15) are expanded in power series in ϵ:

$$T_i = \epsilon T_i^{(1)} + \epsilon^2 T_i^{(2)} + \ldots, \tag{18}$$

$$\psi_i = \epsilon\psi_i^{(1)} + \epsilon^2\psi_i^{(2)} + \ldots. \tag{19}$$

The Rayleigh number R may also be expanded in a finite power series. From (17)

$$R = \frac{R_c}{1-\epsilon^2}$$
$$= R_c + R_c^{(s)}(\epsilon^2 + \epsilon^4 + \ldots + \epsilon^{2s}) \tag{20}$$

where $R_c^{(s)} = R_c/(1-\epsilon^{2s})$. Writing $R_c^{(s)}$ in this fashion ensures that, expanded to a finite order of ϵ, the correct value of R is used. For each layer, we may also expand R_i as

$$R_i = R_{ic} + R_{ic}^{(s)}(\epsilon^2 + \epsilon^4 + \ldots + \epsilon^{2s}), \tag{21}$$

where $R_{ic}^{(s)} = R_{ic}/(1-\epsilon^{2s})$.

The above series for T_i, ψ_i, R_i are substituted in (14), (15) and the boundary conditions, and give rise to a sequence of problems each associated with a power of ϵ.

4. The first-order (onset) problem

By substituting (18), (19) and (21) into (14) and (15), we obtain, for the first-order ($O(\epsilon)$) problem,

$$\frac{\partial^2\psi_i^{(1)}}{\partial X^2} + \frac{1}{r_i^2}\frac{\partial^2\psi_i^{(1)}}{\partial Z_i^2} = -\frac{R_{ic}}{r_i^2}\frac{\partial T_i^{(1)}}{\partial X}, \tag{22}$$

$$\frac{\partial^2 T_i^{(1)}}{\partial X^2} + \frac{1}{r_i^2}\frac{\partial^2 T_i^{(1)}}{\partial Z_i^2} = \frac{\partial\psi_i^{(1)}}{\partial X}, \tag{23}$$

together with the boundary conditions (16) with T_i, ψ_i replaced by $T_i^{(1)}$, $\psi_i^{(1)}$, $i = 1, 2, \ldots, N$. This is the 'onset' problem for convection in a layered medium, previously formulated by McKibbin & O'Sullivan (1980) and briefly outlined here.

The Fourier series expansions of $T_i^{(1)}$, $\psi_i^{(1)}$ consistent with the lateral boundary conditions may be written

$$T_i^{(1)} = \sum_{n=0}^{\infty} T_{in}^{(1)} \cos\frac{n\pi X}{L},$$

$$\psi_i^{(1)} = \sum_{n=1}^{\infty} \psi_{in}^{(1)} \sin\frac{n\pi X}{L},$$

where doubly subscripted variables are functions of Z_i only. Substitution into (22), (23) and matching the coefficients of the orthogonal eigenfunctions gives

$$[D_i^2 - (n\alpha_i)^2]\psi_{in}^{(1)} = n\frac{\alpha_i}{r_i} R_{ic} T_{in}^{(1)}, \tag{24}$$

$$[D_i^2 - (n\alpha_i)^2] T_{in}^{(1)} = n\alpha_i r_i \psi_{in}^{(1)}, \tag{25}$$

where $D_i = d/dZ_i$ and $\alpha_i = \pi r_i/L$, for $i = 1, 2, \ldots, N$ and $n = 0, 1, 2, \ldots$. The boundary conditions are found by a similar matching process. It turns out that the terms $T_{i0}^{(1)}$ are zero. We choose the cell width L of the onset disturbance to be that corresponding to a single cell, that is horizontal wavenumber 1. (The Rayleigh numbers for onset of larger wavenumber components are then higher than for $n = 1$.) Therefore we take $T_{in}^{(1)} = \psi_{in}^{(1)} = 0$ for $n \geqslant 2$, and

$$T_i^{(1)} = T_{i1}^{(1)} \cos\frac{\pi X}{L}, \quad \psi_i^{(1)} = \psi_{i1}^{(1)} \sin\frac{\pi X}{L}.$$

Elimination of either $T_{i1}^{(1)}$ or $\psi_{i1}^{(1)}$ from (24) and (25) (with $n = 1$) gives

$$[(D_i^2-\alpha_i^2)^2-\alpha_i^2 R_{ic}](T_{i1}^{(1)}, \psi_{i1}^{(1)}) = 0.$$

Using (24) and (25) the solutions for $T_{i1}^{(1)}$, $\psi_{i1}^{(1)}$ can be written in the form

$$T_{i1}^{(1)} = A_i^{(1)} \sinh \beta_i Z_i + B_i^{(1)} \cosh \beta_i Z_i + E_i^{(1)} \sinh \gamma_i Z_i + F_i^{(1)} \cosh \gamma_i Z_i, \tag{26}$$

$$\psi_{i1}^{(1)} = \frac{\alpha_i \eta_i}{r_i}(A_i^{(1)} \sinh \beta_i Z_i + B_i^{(1)} \cosh \beta_i Z_i - E_i^{(1)} \sinh \gamma_i Z_i - F_i^{(1)} \cosh \gamma_i Z_i), \tag{27}$$

where $\beta_i = \alpha_i(1+\eta_i)^{\frac{1}{2}}$ and $\gamma_i = \alpha_i(1-\eta_i)^{\frac{1}{2}}$ with $\eta_i = (R_{ic})^{\frac{1}{2}}/\alpha_i$. Note that γ_i may be imaginary or zero with corresponding trigonometric or linear forms in (26) and (27).

Substitution of (26) and (27) into the boundary conditions gives $4N$ homogeneous linear equations in the $4N$ unknown coefficients $A_i^{(1)}$, $B_i^{(1)}$, $E_i^{(1)}$ and $F_i^{(1)}$, $i = 1, 2, \ldots, N$. These equations (see McKibbin & O'Sullivan) can be written in the matrix form

$$\mathbf{M}\mathbf{A}^{(1)} = 0, \tag{28}$$

where $\mathbf{A}^{(1)} = (A_1^{(1)}, B_1^{(1)}, E_1^{(1)}, F_1^{(1)}, A_2^{(1)}, B_2^{(1)}, E_2^{(1)}, F_2^{(1)}, \ldots, A_N^{(1)}, B_N^{(1)}, E_N^{(1)}, F_N^{(1)})^T$ is the vector of first-order coefficients, and $\mathbf{M}$ is a $4N \times 4N$ matrix found from the boundary condition equations. The condition for a non-trivial solution for $\mathbf{A}^{(1)}$ is $\det \mathbf{M} = 0$, which is solved for the variable R_c. The resulting solution for $\mathbf{A}^{(1)}$ may be normalized (in this case we set $E_1^{(1)} = 1{\cdot}0$) and the amplitude of the motion represented by a multiplicative constant a_1. We then write

$$T_i^{(1)} = a_1 \hat{T}_{i1}^{(1)} \cos\frac{\pi X}{L}, \quad \psi_i^{(1)} = a_1 \hat{\psi}_{i1}^{(1)} \sin\frac{\pi X}{L}, \tag{29}$$

where a circumflex denotes a normalized quantity. The value of a_1 is not determined as part of the onset solution but will be found from a 'solvability' condition arising in the third-order problem.

5. The higher-order problems

The solutions for higher-order problems are written in the form

$$T_i^{(k)} = a_k \hat{T}_{i1}^{(1)} \cos\frac{\pi X}{L} + \sum_{n=0}^{\infty} T_{in}^{(k)} \cos\frac{n\pi X}{L}, \tag{30}$$

$$\psi_i^{(k)} = a_k \hat{\psi}_{i1}^{(1)} \sin\frac{\pi X}{L} + \sum_{n=1}^{\infty} \psi_{in}^{(k)} \sin\frac{n\pi X}{L}, \tag{31}$$

where amplitudes a_k may be determined from the order $k+2$ problem.

The $O(\epsilon^2)$ equations are

$$\frac{\partial^2 \psi_i^{(2)}}{\partial X^2} + \frac{1}{r_i^2}\frac{\partial^2 \psi_i^{(2)}}{\partial Z_i^2} = -\frac{R_{ic}}{r_i^2}\frac{\partial T_i^{(2)}}{\partial X}, \tag{32}$$

$$\frac{\partial^2 T_i^{(2)}}{\partial X^2} + \frac{1}{r_i^2}\frac{\partial^2 T_i^{(2)}}{\partial Z_i^2} = \frac{\partial \psi_i^{(2)}}{\partial X} + \frac{\partial \psi_i^{(1)}}{\partial Z_i}\frac{\partial T_i^{(1)}}{\partial X} - \frac{\partial \psi_i^{(1)}}{\partial X}\frac{\partial T_i^{(1)}}{\partial Z_i}, \tag{33}$$

for $i = 1, 2, \ldots, N$ with associated boundary conditions. The expressions (30) and (31) for $T_i^{(2)}$, $\psi_i^{(2)}$ are substituted into (32) and (33). Equating coefficients of the Fourier-series terms in the equations and in the boundary conditions gives non-trivial solu-

tions only for $n = 0$ and $n = 2$. These two problems are solved by a process similar to that for the first-order case, using matrix methods. The resulting expressions for $T_{i0}^{(2)}$ and $T_{i2}^{(2)}$, $\psi_{i2}^{(2)}$ are algebraically complicated, and will not be given here; their important property is that they are proportional to a_1^2.

The expansions for the second-order terms can then be written

$$T_i^{(2)} = a_2 \hat{T}_{i1}^{(1)} \cos\frac{\pi X}{L} + a_1^2 \left(\hat{T}_{i0}^{(2)} + \hat{T}_{i2}^{(2)} \cos\frac{2\pi X}{L}\right), \tag{34}$$

$$\psi_i^{(2)} = a_2 \hat{\psi}_{i1}^{(1)} \sin\frac{\pi X}{L} + a_1^2 \hat{\psi}_{i2}^{(2)} \sin\frac{2\pi X}{L} \tag{35}$$

The third-order problem is found by retaining $O(\epsilon^3)$ terms, and is given by

$$\frac{\partial^2 \psi_i^{(3)}}{\partial X^2} + \frac{1}{r_i^2}\frac{\partial^2 \psi_i^{(3)}}{\partial Z_i^2} = -\frac{R_{ic}}{r_i^2}\frac{\partial T_i^{(3)}}{\partial X} - \frac{R_{ic}^{(s)}}{r_i^2}\frac{\partial T_i^{(1)}}{\partial X}, \tag{36}$$

$$\frac{\partial^2 T_i^{(3)}}{\partial X^2} + \frac{1}{r_i^2}\frac{\partial^2 T_i^{(3)}}{\partial Z_i^2} = \frac{\partial \psi_i^{(3)}}{\partial X} + \frac{\partial \psi_i^{(1)}}{\partial Z_i}\frac{\partial T_i^{(2)}}{\partial X} + \frac{\partial \psi_i^{(2)}}{\partial Z_i}\frac{\partial T_i^{(1)}}{\partial X} - \frac{\partial \psi_i^{(1)}}{\partial X}\frac{\partial T_i^{(2)}}{\partial Z_i} - \frac{\partial \psi_i^{(2)}}{\partial X}\frac{\partial T_i^{(1)}}{\partial Z_i}. \tag{37}$$

After substitution of expressions (30), (31) for $T_i^{(3)}$, $\psi_i^{(3)}$, (34), (35) for $T_i^{(2)}$, $\psi_i^{(2)}$ and (29) for $T_i^{(1)}$, $\psi_i^{(1)}$ into (36) and (37), equating Fourier series coefficients gives non-trivial solutions only for $n = 0$, 1, 2, and 3. The solvability condition for the problem when $n = 1$ gives a relationship between a_1 and $R_c^{(s)}$ as follows.

The equations for the functions $T_{i1}^{(3)}$, $\psi_{i1}^{(3)}$ are found to be

$$(D_i^2 - \alpha_i^2)\,\psi_{i1}^{(3)} = \frac{\alpha_i}{r_i} R_{ic} T_{i1}^{(3)} + \frac{\alpha_i}{r_i} R_{ic}^{(s)} a_1 \hat{T}_{i1}^{(1)},$$

$$(D_i^2 - \alpha_i^2)\,T_{i1}^{(3)} = \alpha_i r_i \psi_{i1}^{(3)} - \alpha_i r_i a_1^3 [\hat{\psi}_{i1}^{(1)} D_i \hat{T}_{i0}^{(2)} + \hat{T}_{i2}^{(2)} D_i \hat{\psi}_{i1}^{(1)} + \tfrac{1}{2}\hat{T}_{i1}^{(1)} D_i \hat{\psi}_{i2}^{(2)} + \tfrac{1}{2}\hat{\psi}_{i1}^{(1)} D_i \hat{T}_{i2}^{(2)} + \hat{\psi}_{i2}^{(2)} D_i \hat{T}_{i1}^{(1)}].$$

Elimination of $T_{i1}^{(3)}$, $\psi_{i1}^{(3)}$ separately gives two fourth-order differential equations, with algebraically complicated non-homogeneous parts. The differential equations and boundary conditions are not self-adjoint and therefore it is difficult to find a solvability condition directly from them. Instead we solve them directly and determine the condition algebraically. Substitution of the (previously found) expressions for the lower-order solutions allows the third-order solutions to be expressed in the form

$$T_{i1}^{(3)} = A_i^{(3)} \sinh\beta_i Z_i + B_i^{(3)} \cosh\beta_i Z_i + E_i^{(3)} \sinh\gamma_i Z_i + F_i^{(3)} \cosh\gamma_i Z_i + a_1 \frac{R_{ic}^{(s)}}{R_{ic}} G_i(Z_i) + a_1^3 H_i(Z_i),$$

$$\psi_{i1}^{(3)} = \frac{\alpha_i \eta_i}{r_i}(A_i^{(3)} \sinh\beta_i Z_i + B_i^{(3)} \cosh\beta_i Z_i - E_i^{(3)} \sinh\gamma_i Z_i - F_i^{(3)} \cosh\gamma_i Z_i) + a_1 \frac{R_{ic}^{(s)}}{R_{ic}} P_i(Z_i) + a_1^3 Q_i(Z_i)$$

for $i = 1, 2, \ldots, N$, where G_i, H_i, P_i, Q_i are known functions of Z_i, calculated in terms of the parameters of the first- and second-order solutions.

Use of the boundary conditions leads to a set of $4N$ non-homogeneous linear

equations in the $4N$ unknown coefficients $A_i^{(3)}$, $B_i^{(3)}$, $E_i^{(3)}$ and $F_i^{(3)}$, $i = 1, 2, \ldots, N$. These equations can be written in matrix form

$$\mathbf{M}\mathbf{A}^{(3)} = a_1\left(\frac{R_c^{(s)}}{R_c}\mathbf{G} + a_1^2\mathbf{H}\right), \tag{38}$$

where $\mathbf{A}^{(3)} = (A_1^{(3)}, B_1^{(3)}, E_1^{(3)}, F_1^{(3)}, A_2^{(3)}, B_2^{(3)}, E_2^{(3)}, F_2^{(3)}, \ldots, A_N^{(3)}, B_N^{(3)}, E_N^{(3)}, F_N^{(3)})^T$, $\mathbf{M}$ is the $4N \times 4N$ matrix found in the first-order problem (see equation (28)) and $\mathbf{G}$ and $\mathbf{H}$ are known vectors. (Use is made of the relationship $R_{ic}^{(s)}/R_{ic} = R_c^{(s)}/R_c$ for $i = 1, 2, \ldots, N$.) However, it is known that $\det \mathbf{M} = 0$. The condition that (38) represents a compatible set of equations and hence is solvable to within a multiplicative constant a_3 leads to a relationship between $R_c^{(s)}/R_c$ and a_1^2. This may be written

$$a_1^2 = \theta R_c^{(s)}/R_c, \tag{39}$$

where θ depends on the number of layers, layer depths, layer permeability and conductivity ratios, cell-width and the upper surface boundary condition for the system under consideration.

6. The Nusselt number

The complexity of the algebra involved in calculating higher-order solutions prevents this approach being used to find those components. However, at this stage we are able to calculate a second-order approximation for the Nusselt number Nu.

Since we are truncating the perturbation expansion at this order we put $s = 1$ in (20) and, rearranging, obtain

$$\epsilon^2 \frac{R_c^{(1)}}{R_c} = \frac{R}{R_c} - 1. \tag{40}$$

The Nusselt number, Nu, from (13) is, to $O(\epsilon^2)$:

$$\begin{aligned} Nu &= \frac{1}{L}\int_0^L \left(1 - \epsilon\frac{\partial T_1^{(1)}}{\partial Z_1} - \epsilon^2\frac{\partial T_1^{(2)}}{\partial Z_1}\right)_{Z_1=0} dX \\ &= 1 + \epsilon^2 a_1^2\left(-\frac{d\hat{T}_{10}^{(2)}}{dZ_1}\right)_{Z_1=0} \end{aligned}$$

after substitution of the expressions for $T_1^{(1)}$ and $T_1^{(2)}$.

From (39), $a_1^2 = \theta R_c^{(1)}/R_c$ and then (40) gives

$$Nu = 1 + \sigma\left(\frac{R}{R_c} - 1\right), \tag{41}$$

where

$$\sigma = \theta\left(-\frac{d\hat{T}_{10}^{(2)}}{dZ_1}\right)_{Z_1=0}$$

is now known. The expression (41) for Nu gives the relationship between the Rayleigh number R and the heat flow through a layered system, for $R > R_c$. Expression of Nu in this form enables a direct comparison to be made with the value for a homogeneous layer with an impermeable top. For the latter case, $Nu_c = 1$, and $Nu = 1 + 2(R/R_c - 1)$ for $R > R_c$, which is the result given by Palm *et al.* (1972) in their equation (3.19), after using (3.4) with $s = 1$.

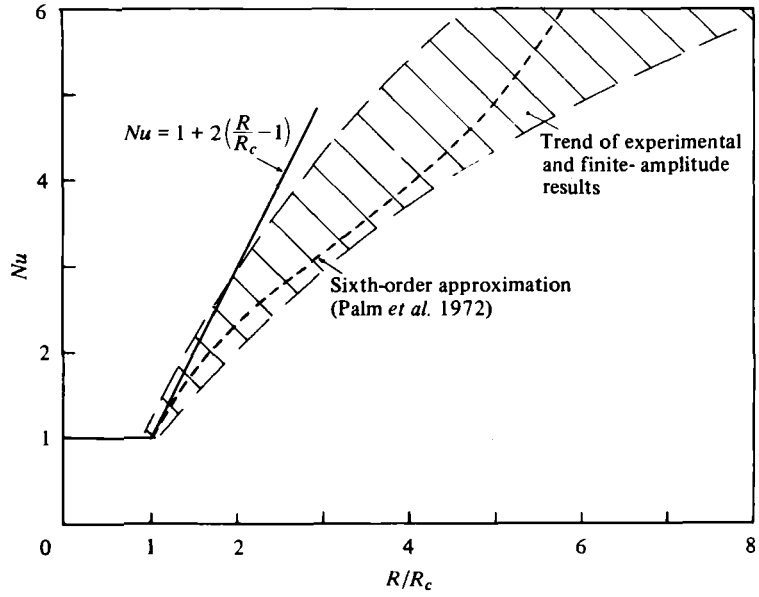

FIGURE 2. Nusselt number Nu for a homogeneous layer with a closed top.

7. Numerical results

There are clearly a wide variety of possible configurations and values of the various parameters used; thus only a small proportion of possible results can be presented here. Also there have been very few finite-amplitude numerical results and no experimental values reported for multi-layer systems, to enable comparison with results found in the present study. The presentation of a small selection of values will probably provide a better source for quantitative and, perhaps more importantly, qualitative comparisons than a large number of detailed results. Consequently, analysis is confined to the two- and three-layer cases, and in particular to a permeable aquifer either overlain ('capped') by, or overlying, a less permeable layer, or lying centrally between two layers of another permeable material. These are then compared with results for a homogeneous layer with either a closed (case A) or an open (case B) upper surface.

Since the emphasis is chosen to be on the different permeabilities of the layers, the conductivities (and hence thermal diffusivities) of all the layers are assumed to be equal in what follows, i.e. $k_i = k_1$, $i = 2, \ldots, N$. (Results for layers of different conductivities may easily be found in the same way as those given below.)

The behaviour of any particular layered system will thus depend on the layer depths r_i, the permeability ratios K_i/K_1, the upper boundary conditions, and, in the case where there are lateral boundaries, on the distance between them. Both the laterally unbounded and bounded cases can be treated simultaneously by considering the behaviour of one cell only, of width L. The criterion used to determine the cell-width at onset in either system is that the value of R_c should be a minimum with respect to L.

For each layered configuration, calculation of the critical value of R, which is a scaled Rayleigh number based on the parameters K_1, k_1 of the bottom layer, enables

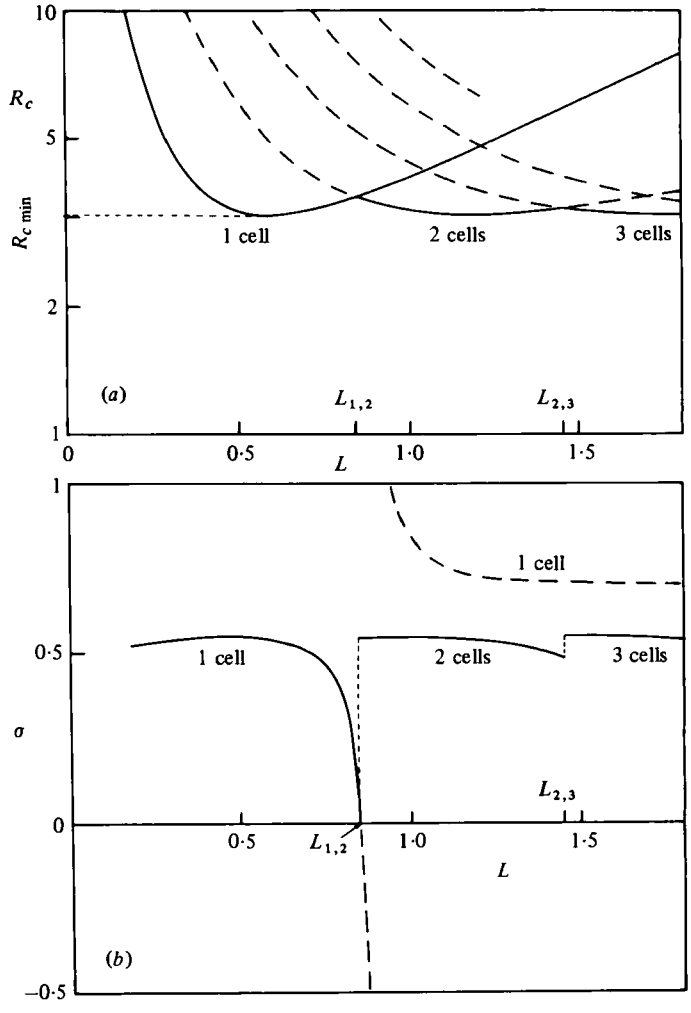

FIGURE 3. Variation of R_c and σ with system width for the two-layer system $r_1 = 0{\cdot}5$, $k_2/k_1 = 1{\cdot}0$, $K_2/K_1 = 0{\cdot}01$, closed top. (*a*) R_c *vs.* L; (*b*) σ *vs.* L.

a comparison to be made of the temperature difference required for onset of convection in the system with that required for a laterally unbounded homogeneous layer composed completely of the material of the bottom layer for the stratified case. The associated value of L then gives the cell-width of the two-dimensional rolls of the convection pattern at onset in the layered system. The subsequently calculated number σ gives the slope of the graph of the Nusselt number Nu versus R/R_c for values of R above R_c.

The graph of Nu for each layered system will be similar in form to that for the homogeneous layer with a closed top (where the minimum critical value of R is $R_c = 1{\cdot}0$ with $L = 1{\cdot}0$ and $\sigma = 2{\cdot}0$), shown in figure 2. The best higher-order approximation found by Palm *et al.* for a single cell of width 1·0 is also shown on this graph, together with the trend indicated by experimental and finite-amplitude results for an unbounded layer. The limitations of the first approximation in this case are clear.

However, for values of R near R_c, prediction of Nu with this first approximation is close enough to show that the results for the layered cases will be a useful indication of the heat flux for values of R not too far above R_c.

In general, the results for any particular system follow a pattern which can be best described by taking an example. We choose as this example the two-layer configuration with $r_1 = 0{\cdot}5$, $K_2/K_1 = 0{\cdot}01$ and with a closed top (case A), results for which are given in figure 3.

Variation in the width L of the cell produces variation of the critical Rayleigh number R_c at which onset of convection can occur (see figure 3a). For a narrow cell, R_c is large; as the width of the confined cell increases, R_c first decreases to a minimum value $R_{c\min}$ (this corresponds to the previously defined criterion for onset in an unbounded system) and then begins to increase again. The results for one cell may be used to determine those for larger numbers of cells, by appropriate scalings of the single-cell curve, and superposing them – the resulting curves are shown as broken lines in figure 3(a). At some larger value of L, which we denote $L_{1,2}$, the value of R_c corresponding to the formation of two cells side by side, each of width $\frac{1}{2}L_{1,2}$, becomes equal to that for the formation of one cell. As the total width of the system is increased above $L_{1,2}$ two cells become the preferred onset pattern, and at still larger widths (denoted $L_{2,3}$, $L_{3,4}$ etc.) it can be seen that larger numbers of cells will form, the number of cells being determined by choosing the curve which minimizes R_c with respect to the total system width.

The corresponding variation in the value of σ, shown in figure 3(b), is interesting. After rising to a maximum value, σ decreases with increasing L and becomes exactly zero at $L_{1,2}$ where the one cell/two cell change takes place. For a single cell and values of L above $L_{1,2}$, σ continues to decrease, first becoming negative, and then discontinuously positive, with moderate values as L becomes large. These latter values of σ for $L > L_{1,2}$ may have no physical significance, however, since at $L = L_{1,2}$ the preferred onset pattern changes to two cells and σ changes (discontinuously) from zero to that value corresponding to $L = \frac{1}{2}L_{1,2}$. At a Rayleigh number above the critical values for both one cell and two cells it may be possible to induce either mode with the right choice of initial disturbance. However for cell-widths for which σ is negative it seems likely that a single wide cell is physically unrealizable. Further finite-amplitude investigations are required for complete understanding of this point. By superposing the scaled multi-cell curves in the same way as for R_c in figure 3(a), it is seen that similar discontinuities in the graph of σ occur at each width $L_{n,n+1}$ where a change from n cells to $n+1$ cells takes place, although, for $n > 1$, the value of σ does not decrease to zero at the changeover width (see figure 3b).

At supercritical Rayleigh numbers the cell-width of the convection cells is often determined by the maximum heat flux principle (first postulated by Malkus 1954). However there are two points which need to be considered in applying this principle. Firstly the Nusselt number, given by $Nu(L) = 1 + \sigma(L)\,(R/R_c(L) - 1)$ does not necessarily attain its maximum at the same value of L which minimizes R_c. Certainly it can be seen from figure 3(b) that σ is not a maximum at the cell-width for which R_c takes its absolute minimum $R_{c\min}$. Thus as R increases beyond its value $R_{c\min}$ at onset the cell-width for maximum heat transfer may change. Secondly it has been shown by Straus & Schubert (1979) that the maximum heat transfer principle is not strictly correct. For a uniform layer at low supercritical Rayleigh numbers three-

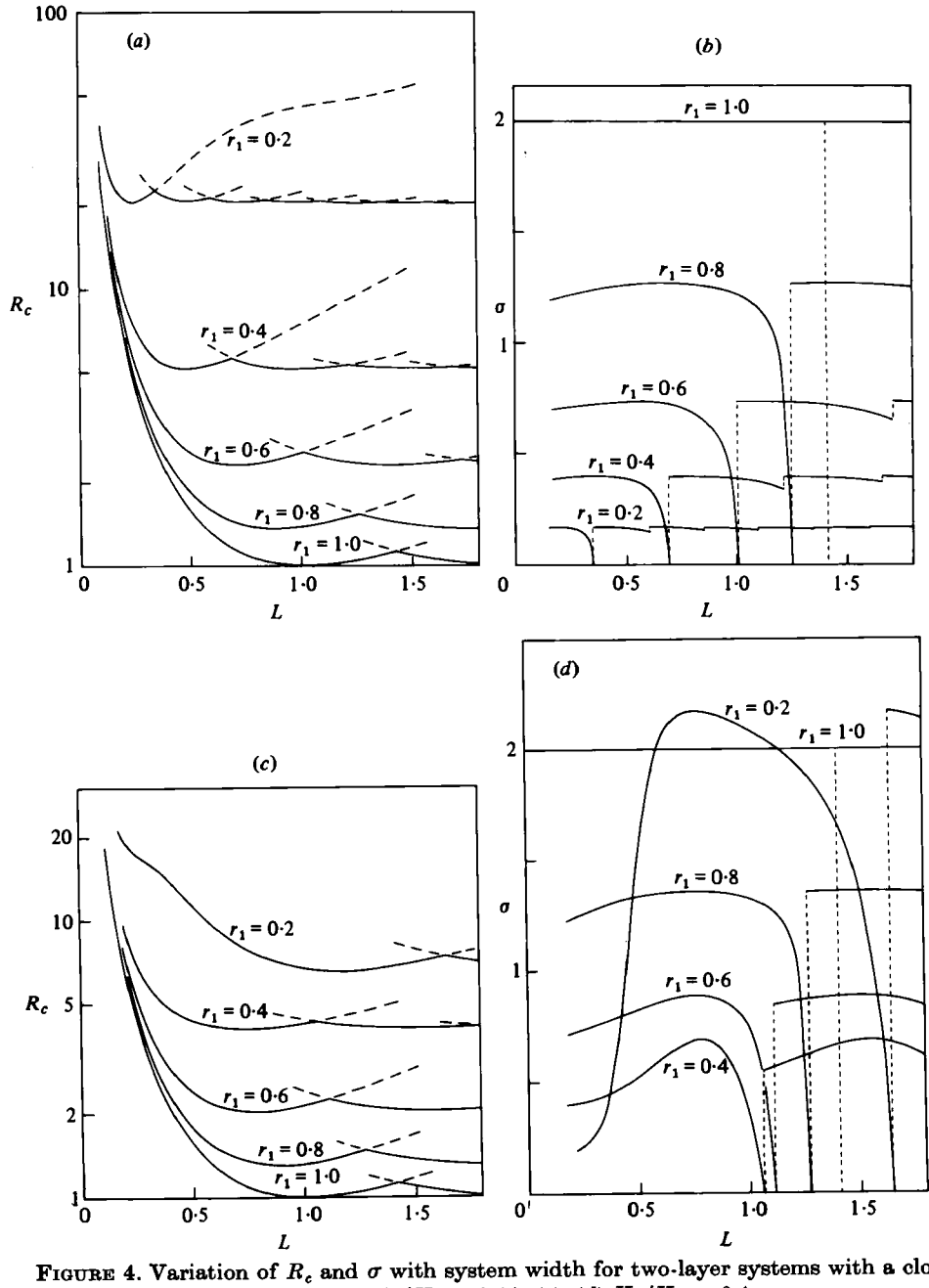

FIGURE 4. Variation of R_c and σ with system width for two-layer systems with a closed top. (*a*), (*b*) $K_2/K_1 = 0{\cdot}01$; (*c*), (*d*) $K_2/K_1 = 0{\cdot}1$.

dimensional flow transports less heat than a two-dimensional roll but random initial conditions may lead to either state. These authors suggest that the lack of clear preference may reflect the fact that the Nusselt numbers for both modes of convection are close.

These points are further discussed in §9 particularly with respect to the occurrence of more than one two-dimensional convection mode.

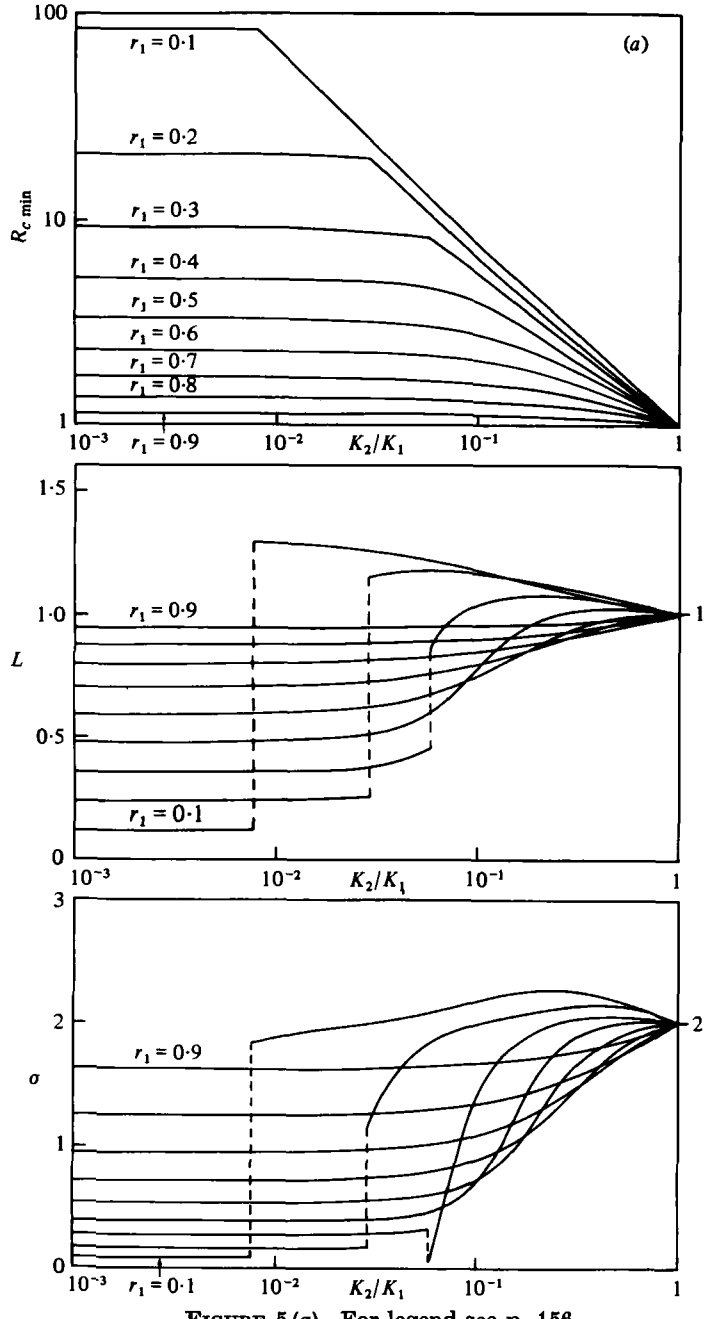

FIGURE 5 (*a*). For legend see p. 156.

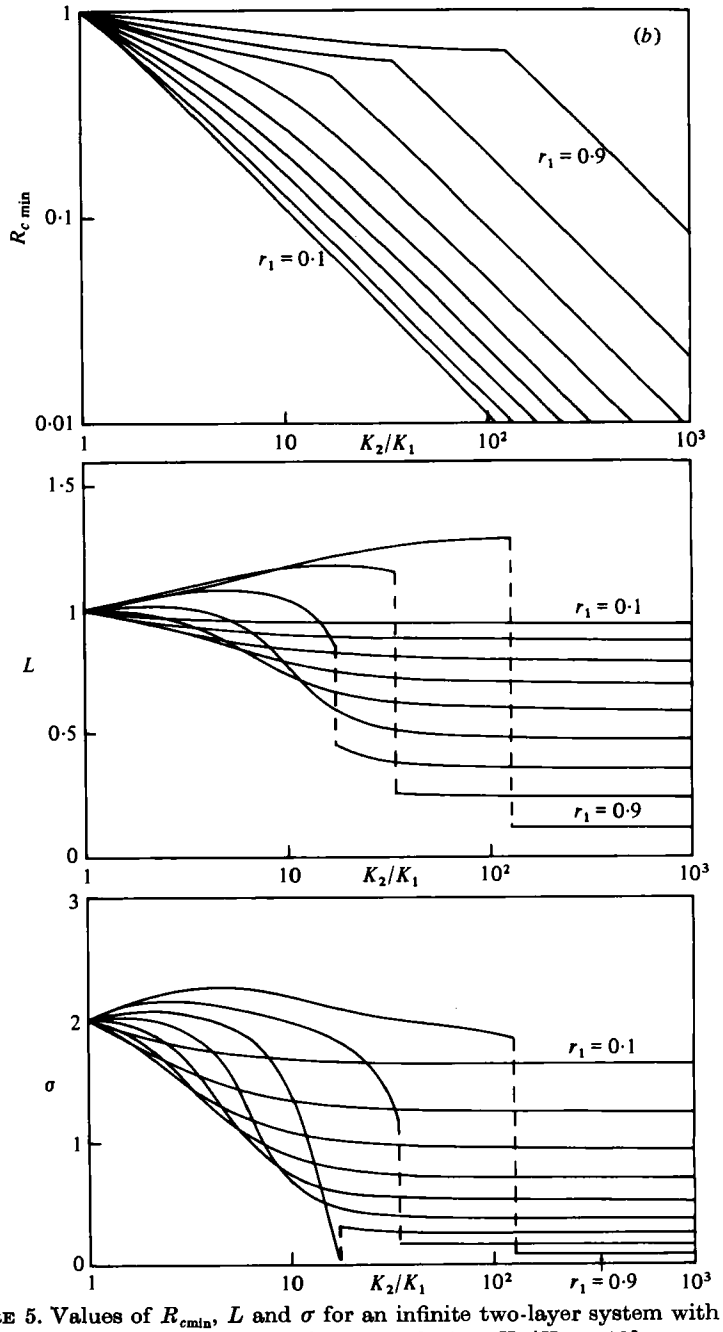

FIGURE 5. Values of R_{cmin}, L and σ for an infinite two-layer system with a closed top. (*a*) $10^{-3} \leqslant K_2/K_1 \leqslant 1$; (*b*) $1 \leqslant K_2/K_1 \leqslant 10^3$.

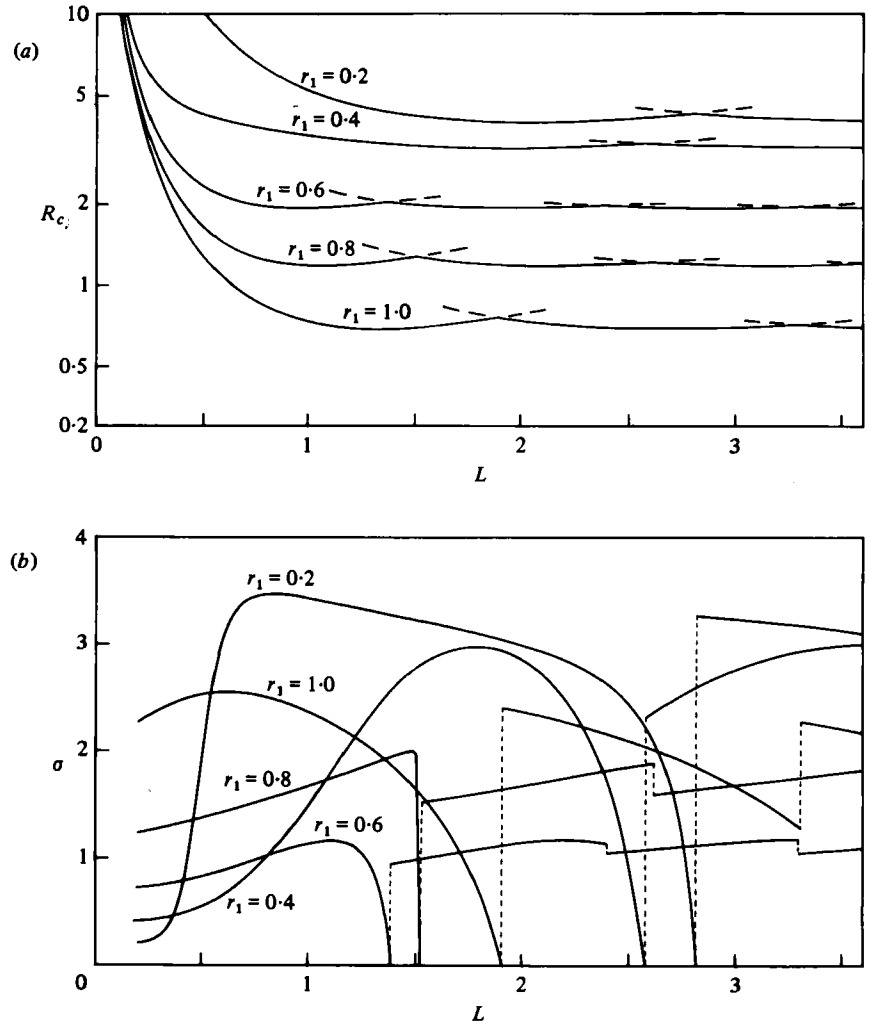

FIGURE 6 (*a*, *b*). For legend see p. 158.

8. The two-layer system

(*a*) *Closed top* (*case A*)

A summary of some results for two-layer systems with a closed top (impermeable upper boundary) for $K_2/K_1 = 0{\cdot}01$ and $0{\cdot}1$ and for $r_1 = 0{\cdot}2(0{\cdot}2)1{\cdot}0$ are shown in figure 4. The values for R_c are determined, as described above, by the criterion that the critical Rayleigh number for the system be minimized with respect to the system width L; consequent discontinuities in the value of σ occur at the changeover values, where the preferred number of cells at onset increases by one. The pattern for each set of parameters can be seen to be similar to the particular case discussed in §7.

There is, however, one exception to this general rule, and a major one at that. The case of a homogeneous system (that is where no layering is present, given in figure 4 by the values for $r_1 = 1{\cdot}0$) has, to the order of the analysis presented here, no variation

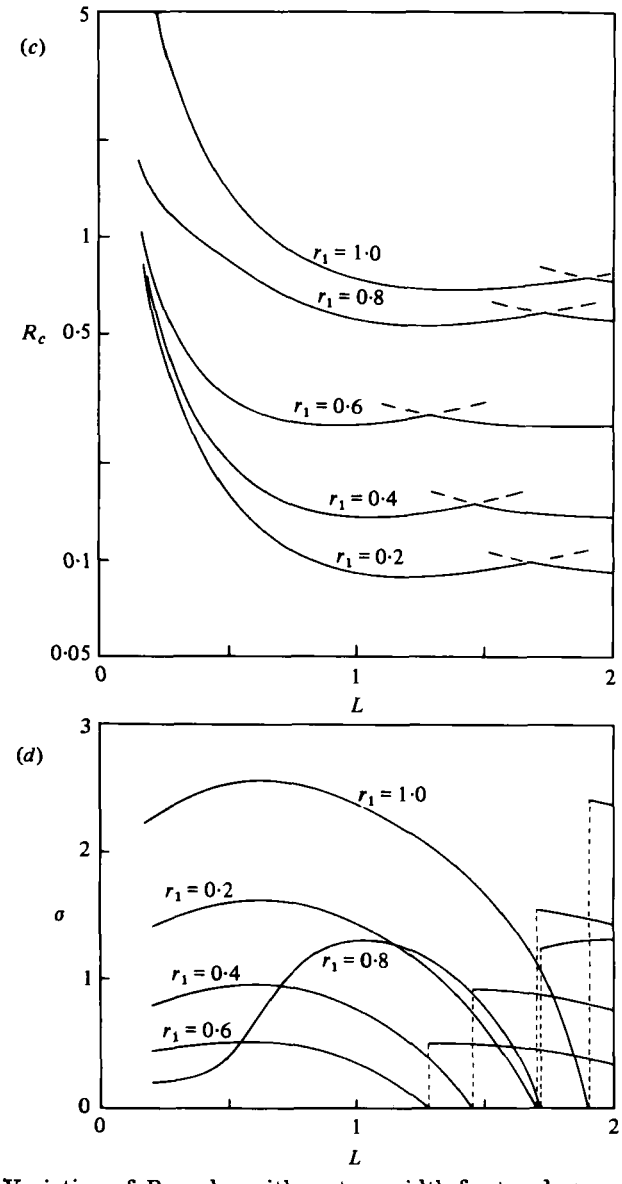

FIGURE 6. Variation of R_c and σ with system width for two-layer systems with an open top. (*a*), (*b*) $K_2/K_1 = 0{\cdot}1$; (*c*), (*d*) $K_2/K_1 = 10$.

of σ with cell-width L, the value remaining a constant $\sigma = 2{\cdot}0$. Thus σ does not change at $L_{1,2}$ nor at any value $L_{n,n+1}$ where the number of cells increases. This property of a homogeneous layer has not been noted previously (Palm *et al.* considered only a cell with width $L = 1{\cdot}0$). The importance of this exception to the general rule for other layered systems (and also for the homogeneous layer with an open, or constant pressure top (see below)) may be seen in the fact that it is the classic problem which has attracted most research to date. It has often been studied as the simplest model for a geothermal system. The above results indicate that the characteristics of

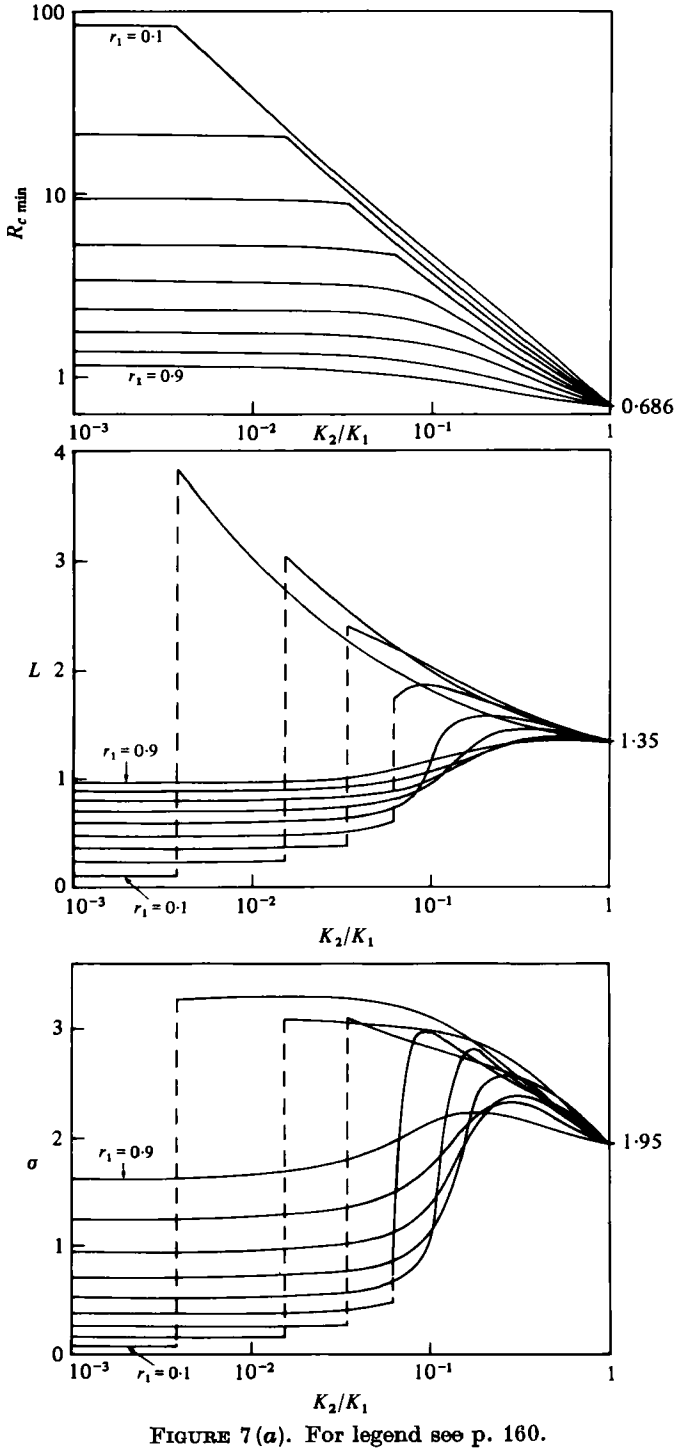

FIGURE 7 (*a*). For legend see p. 160.

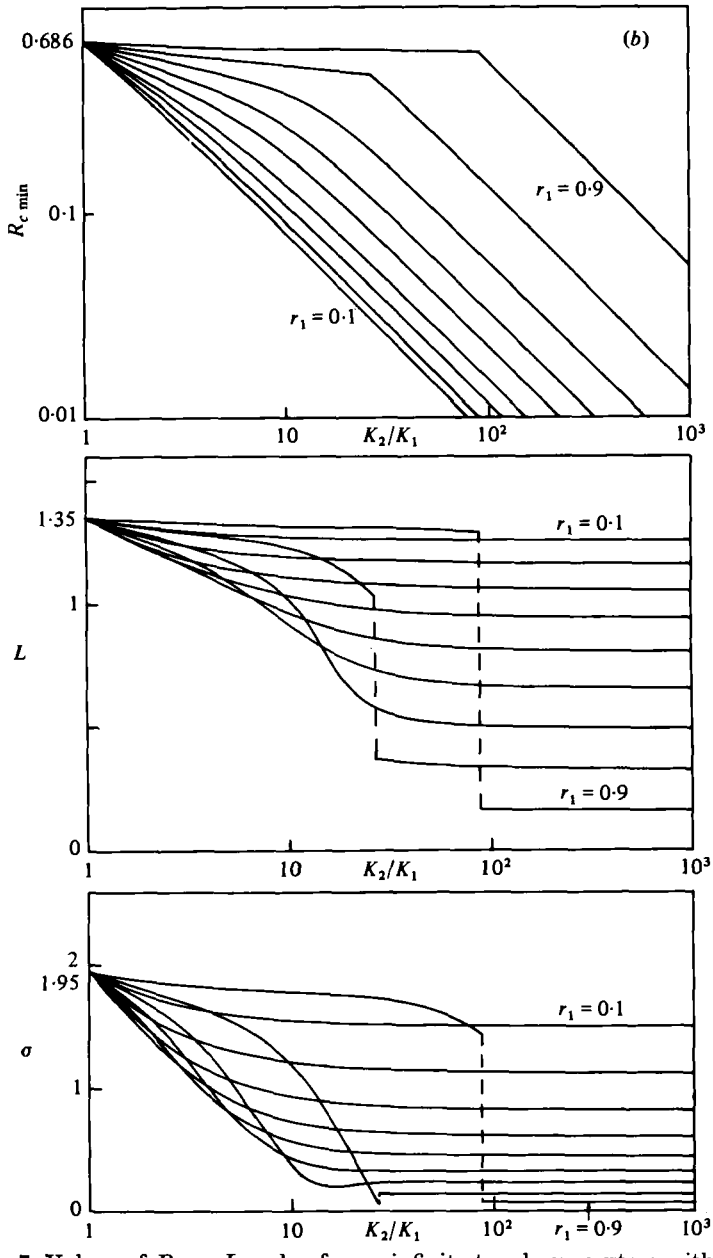

FIGURE 7. Values of R_{cmin}, L and σ for an infinite two-layer system with an open top. (*a*) $10^{-3} \leqslant K_2/K_1 \leqslant 1$; (*b*) $1 \leqslant K_2/K_1 \leqslant 10^3$.

heat transfer for this simple model may be different from those for layered systems in general. The simplicity of that model may therefore mask certain heat-transport properties of water-saturated geothermal systems, which are not homogeneous in configuration.

For the general case, then, σ becomes zero at $L = L_{1,2}$. For a lateral boundary separation slightly less than $L_{1,2}$, σ is very small, and the formula for the heat transfer

(41) shows that there is very little increase in Nu as R initially increases above R_c. The near-maximum-width cell is thus in a somewhat strained state and convects very little heat, even though forced by increased temperature differences. For a system-width slightly greater than $L_{1,2}$, σ is much larger, and the double-cell pattern will convect heat much more readily as R increases above R_c.

As the distance between the lateral boundaries becomes large, the average cell-width approaches that corresponding to the unbounded system result, while the 'changeover' value of R_c for each extra cell becomes closer to the absolute minimum value, $R_{c\min}$, for the single cell. The values of $R_{c\min}$ and corresponding L and σ for an unbounded two-layer system with a closed top are given in figure 5 for

$$10^{-3} \leqslant K_2/K_1 \leqslant 10^3, \quad r_1 = 0{\cdot}1(0{\cdot}1)0{\cdot}9.$$

As explained in McKibbin & O'Sullivan (1980), examination of the dependence of R_c on cell-width L shows that for some configurations there are two local minima. The bifurcations in the graphs in figure 5 result from the changeover as either one or the other of these local minima becomes the absolute minimum. The corresponding cell-widths and the values of σ associated with the two minima are different – an example of a configuration for which this occurs will be discussed further in §9.

(*b*) *Open top* (*case B*)

Results for a two-layer system with a constant-pressure upper boundary condition are similar to the examples given above. The homogeneous layer with an open top also follows the general pattern; unlike the closed-top case, where the value of σ does not vary with L but remains constant at $\sigma = 2{\cdot}0$, the open-top values *do* vary with L (these are given by the curves for $r_1 = 1{\cdot}0$ in the results to follow).

In figure 6, the variation of R_c and σ with system width are given for the cases $K_2/K_1 = 0{\cdot}1$ and $10{\cdot}0$, and $r_1 = 0{\cdot}2(0{\cdot}2)1{\cdot}0$. The values of R_c are found to be lower than the corresponding closed-top cases; this means that the critical temperature difference required to destabilize such a system is less than that for the closed-top case.

The variation of $R_{c\min}$, L and σ with the permeability ratio K_2/K_1 for a laterally unbounded system is given in figure 7 in the same way as for the closed-top case. In particular, for a 'capped' aquifer ($K_2/K_1 < 1$) the cell-widths may be very large (for small r_1, cells may have widths twice or more times the depth). It appears that the wide cell is necessary for circulation of fluid entering the system from above, a greater area of the less permeable material being required to provide enough fluid to pass through the more permeable material beneath while being heated at the base, before being driven upwards again and out of the surface. In physical terms this means that the recharge and discharge areas of such a geothermal system may be a distance apart several times that of the depth of the heater. When the upper layer is too impermeable, however, it transfers heat mainly by conduction, while the fluid convects in smaller closed cells in the more permeable lower layer. For the wide-cell recharge/discharge system, the values of σ are correspondingly large (1·5 or more times that for the homogeneous layer) while being fairly small for the narrow-cell case where the upper layer acts mainly as a conducting medium.

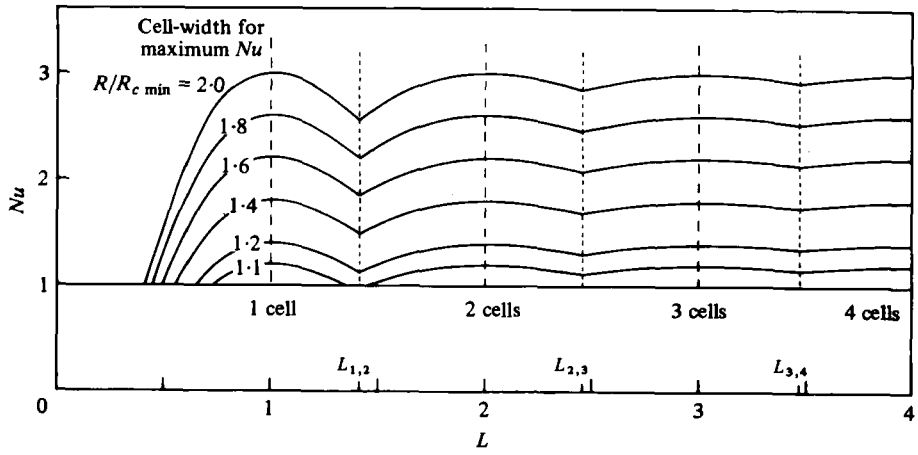

FIGURE 8. Variation of Nu with system width for $R > R_{cmin}$ for a homogeneous layer with a closed top.

9. Variation of Nusselt number with cell width

As noted by Combarnous & Bories (1975) and others, numerical studies of steady finite-amplitude convection show that the heat transfer through a homogeneous layer, bounded horizontally by impervious isothermal surfaces, varies at supercritical Rayleigh numbers with the width of the convecting cells. As discussed earlier in §7 one criterion used for deciding what form the convection pattern at such Rayleigh numbers takes is that the heat flow be maximized, and the cell-width is chosen accordingly; it is found that the widths thus chosen decrease with increasing Rayleigh number. Some justification for this criterion is provided by experimental evidence which shows that, as the Rayleigh number increases, narrower cells form. At slightly supercritical Rayleigh numbers, however, the cell-widths remain close to 1·0, the preferred cell-width at onset of convection.

The present theory can account for the last result, and provides an insight into the behaviour of other systems. The procedure is as follows: for values of R not too far above the minimum critical value R_{cmin} for a given configuration, Nu may be calculated, using (41), as a function of the width of the system, using the values of R_c and σ determined by the overlaid graphs such as in figures 3, 4 and 6. The cell-width which maximizes Nu can then be determined.

As mentioned in the previous section, it is found that the homogeneous closed-top case is unique, in that σ does not vary with cell-width; some values of Nu for $R > R_{cmin} = 1{\cdot}0$ are shown in figure 8. It can be seen that Nu remains maximized by the same cell-width as that corresponding to the onset value of R_c, namely 1·0. A similar result would also hold for any case where the variation of σ with cell-width is either constant, or where σ is at a maximum for the lowest value of R_c. If this is not so, i.e. σ is either increasing or decreasing where R_c is a minimum, then the value of L at which Nu is a maximum increases or decreases respectively as R increases. It should be noted here that, firstly, we have found no case other than the closed-top homogeneous layer where σ, to the present order of analysis, is a constant function of cell-width; second, the maximum for σ does not, in general, correspond exactly to the

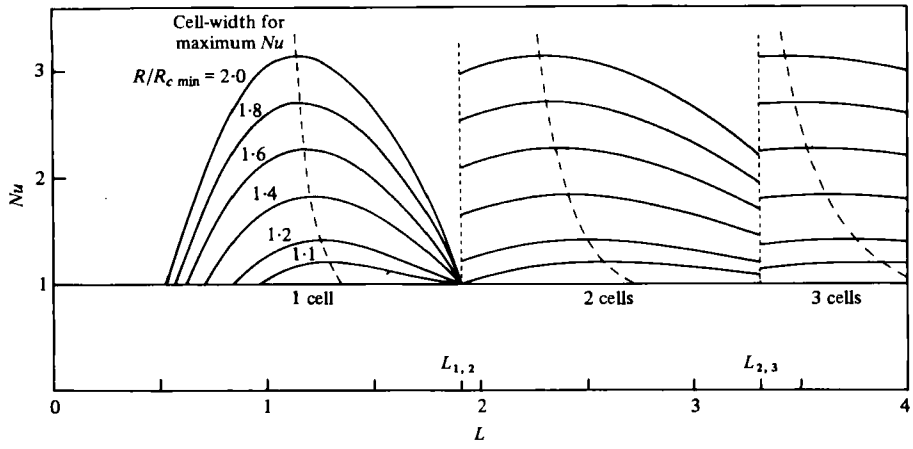

FIGURE 9. Variation of Nu with system width for $R > R_{cmin}$ for a homogeneous layer with an open top.

minimum value of R_c (although in many cases the corresponding two values of L are close).

For the homogeneous layer, one of the authors (O'Sullivan 1980, in an unpublished paper) has shown that Nu does depend on L at $O(\epsilon^4)$, a result which is confirmed by the numerical results of Combarnous & Bories (1975).

One other result which is unique to this case is that at the system widths $L_{n,n+1}$ where the changeover from n cells to $n+1$ cells takes place, the values of Nu for a particular R are continuous. This property does not hold for any other configuration.

The homogeneous layer with a constant-pressure top is a suitable case for amplification and clarification of these and previous comments. The minimum value of R_c is 0·686 (corresponding to an unscaled Rayleigh number of 27·1) at a cell-width $L = 1{\cdot}35$, with $\sigma = 1{\cdot}95$ (see figure 6, curves for $r_1 = 1{\cdot}0$). However, calculation of σ with increasing cell-width gives values which first increase to a maximum of 2·55 at $L = 0{\cdot}63$, and then decrease to zero at $L = 1{\cdot}91$. (This latter value is $L_{1,2}$, the system width at which the critical value R_c for two cells is equal to that for one cell ($R_c = 0{\cdot}758$).) Thus at $L = L_{1,2} = 1{\cdot}91$, the preferred onset mode becomes two cells, and the value of σ increases discontinuously from zero to the value corresponding to a single cell of width $L = \frac{1}{2}L_{1,2} = 0{\cdot}955$, namely $\sigma = 2{\cdot}40$.

In the same way as for the closed-top case above, values of Nu may be calculated for R slightly above the minimum critical value $R_{cmin} = 0{\cdot}686$. Because of the decreasing behaviour of σ at $L = 1{\cdot}351$, the maximum value of Nu does not occur at this value for $R > R_{cmin}$. The graphed values in figure 9 show how Nu is maximized by a cell-width which decreases as R increases. Also there are discontinuities in the values of Nu at each $L_{n,n+1}$.

Results for all the multi-layered systems investigated are similar to those for the open-top homogeneous layer; the discontinuities in σ at $L_{n,n+1}$ cause similar discontinuities in the values of Nu at those system widths. The cell-width which maximizes Nu varies with increasing R to a greater or lesser extent depending on the rate of variation of σ with L near the minimum value of R_c. (In a few cases, the cell-width which maximizes Nu actually increases as R increases.) The effect seems generally greater in systems with an open top. However, to show that multi-layered closed-top

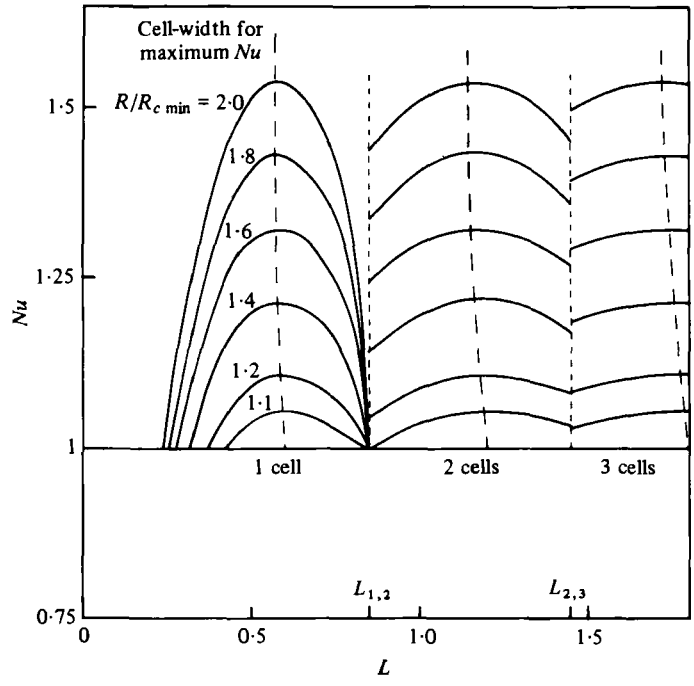

FIGURE 10. Variation of Nu with system width for $R > R_{c\min}$ for the two-layer configuration $r_1 = 0{\cdot}5$, $K_2/K_1 = 0{\cdot}01$, closed top (values of R_c and σ for this case are given in figure 3).

systems also exhibit similar properties, we complete our initial demonstration example (two layers, $r_1 = 0{\cdot}5$, $K_2/K_1 = 0{\cdot}01$, closed top). The graphs of R_c and σ as functions of L were given in figure 3. Figure 10 now shows values of Nu as in the previous two homogeneous-layer cases.

The foregoing examples serve to demonstrate that, to the present order of analysis, the homogeneous closed-top case remains unique. All other configurations show, if Malkus' criterion is used, that the preferred cell-width for flows at even slightly supercritical Rayleigh numbers in a laterally unbounded layer will be different from that corresponding to the onset condition.

Two minima for R_c

As previously noted, for some configurations the graph of R_c as a function of cell-width L has two minima. Generally the values of σ corresponding to these two minima are different. (Some examples corresponding to points where the two minimum values for R_c are equal, are given at the discontinuities in figures 5 and 7.) We present in figure 11 the results for one particular example, namely a two-layer system with $r_1 = 0{\cdot}2$, $K_2/K_1 = 0{\cdot}03$ and a closed top. The values of R_c, calculated for a single cell, are scaled and overlaid for multi-cell flows in the same way as before, to determine the multi-cell change-over widths $L_{n,m}$ for the system. It is evident that the preferred number of cells at onset does not simply increase by one at every changeover value $L_{n,m}$, although, as the system width becomes very large, that part of the curve which corresponds to the smaller of the two minima predominates, and the associated cell-width approaches the laterally unbounded result.

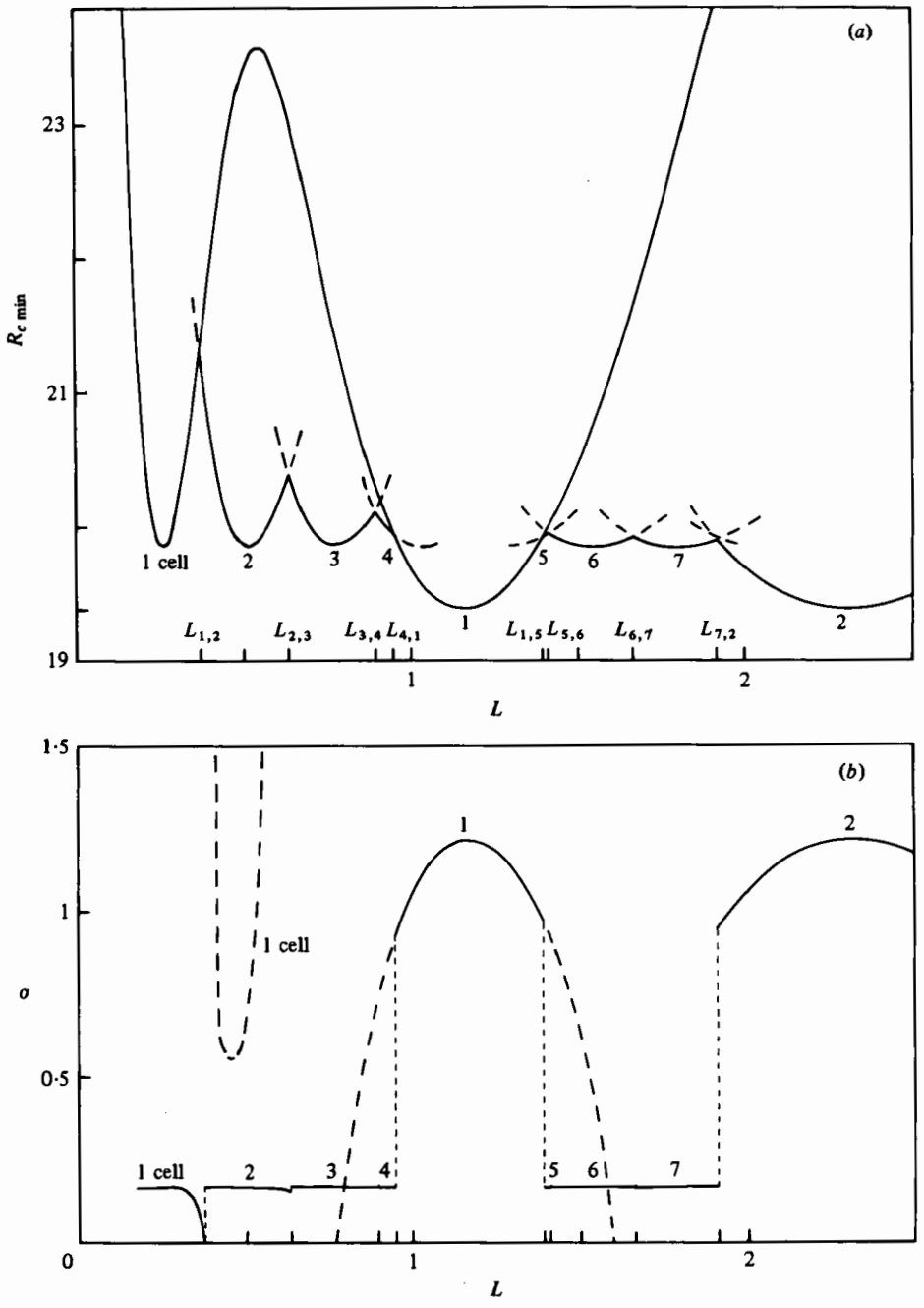

FIGURE 11 (*a*, *b*). For legend see p. 166.

For the case being described, $R_{c\min} = 19{\cdot}38$ ($L = 1{\cdot}16$, $\sigma = 1{\cdot}43$) while, at the other minimum, $R_c = 19{\cdot}85$ ($L = 0{\cdot}26$, $\sigma = 0{\cdot}17$). Some aspects of the behaviour of the graph of σ are similar to that for the case where there is a single minimum for R_c. At $L_{1,2}$ the single-cell value of σ becomes zero; near the minimum at $L = 1{\cdot}16$, σ first increases and then decreases – it again becomes exactly zero at the point where a

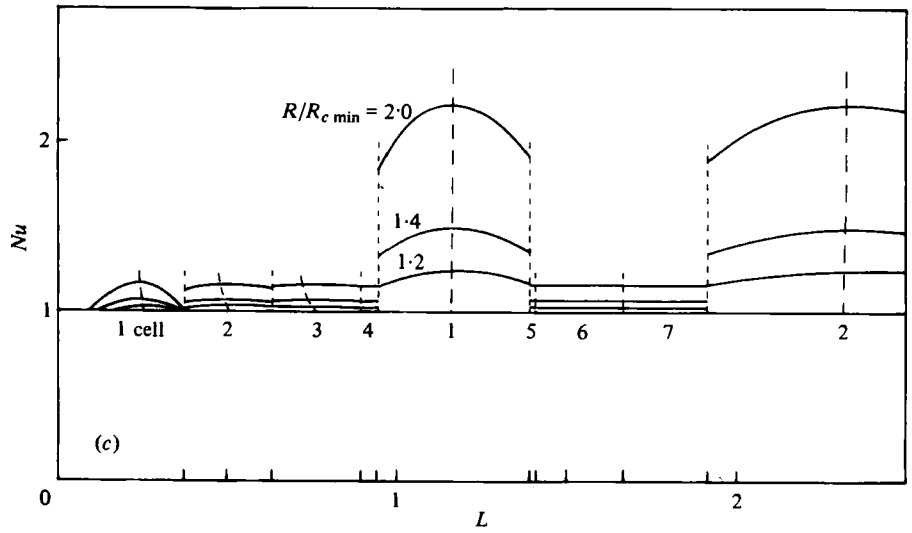

FIGURE 11. Variation of R_c, σ and Nu (for $R > R_{c\min}$) for a configuration where there are two local minima for R_c – a two-layer system with $r_1 = 0{\cdot}2$, $K_2/K_1 = 0{\cdot}03$, closed top.

change from one cell to two cells would take place if those parts of the curves corresponding to multi-cell flows with the smaller cell-width were not present. Figure 11 (*a*) shows the values of R_c as determined by superposition, and figure 11 (*b*) the corresponding values of σ. The higher σ values associated with the greater cell-width indicate greater convective heat transfer than for the smaller cell-width. This is demonstrated in figure 11 (*c*) which shows values of Nu calculated for some supercritical Rayleigh numbers $R > R_{c\min}$. The cell-width which maximizes Nu for the regions corresponding to the narrower cells ($L < L_{4,1}$ and $L_{1,5} < L < L_{7,2}$) decreases as R increases, while, for the regions corresponding to the wider cells, the opposite occurs, although there the increase in cell-width with R is only small.

Which mode is preferred?

An important point that arises here is that onset of convection in a system may not necessarily occur in that mode which will transfer the most heat at higher Rayleigh numbers. For the last example, a lateral boundary separation of 1·5 indicates that, at onset of convection, which occurs at $R = R_c = 20{\cdot}12$, 6 cells will form, each of width 0·25 (i.e. $n = 6$), with the value of σ being 0·17. However the critical Rayleigh number for a single cell of width 1·5 is $R_c = 20{\cdot}50$, with $\sigma = 0{\cdot}62$. For a Rayleigh number $R = 22$, for example, the value of the Nusselt number for the 6-cell convection pattern is, using (41), $Nu_6 = 1{\cdot}016$ while, for the single-cell pattern, $Nu_1 = 1{\cdot}045$. In fact, it may be easily shown by using (41) for each case, that the preferred onset convection pattern (corresponding to the smallest critical Rayleigh number) convects less heat for $R > 20{\cdot}65$ than the single-cell pattern (i.e. $Nu_6 < Nu_1$). For all but the special homogeneous closed top case, similar anomalies exist. For example, in a homogeneous open-top layer, with a lateral boundary separation of 1·6, the formula for the Nusselt number for a single cell (the preferred onset pattern) is

$$Nu_1 = 1 + 1{\cdot}44(R/R_c - 1) \quad \text{for} \quad R > R_c = 0{\cdot}703,$$

while for a two-cell pattern, with each cell of width 0·8,

$$Nu_2 = 1 + 2{\cdot}51(R/R_c - 1) \quad \text{for} \quad R > R_c = 0{\cdot}858.$$

For $R = 0{\cdot}90$, $Nu_1 = 1{\cdot}40$ and $Nu_2 = 1{\cdot}12$, giving $Nu_1 > Nu_2$. But, for $R = 1{\cdot}40$, $Nu_1 = 2{\cdot}43 < Nu_2 = 2{\cdot}59$. For this case it is found that $Nu_1 < Nu_2$ for $R > 1{\cdot}22$.

It may be possible that, at higher Rayleigh numbers, the onset convection pattern is displaced by another pattern that produces the maximum heat flow, although (as indicated by our first example) this need not necessarily lead to narrower cells. The results obtained by Straus & Schubert (1979) for a uniform layer where two- or three-dimensional flows have numerically close Nusselt numbers show that either mode can result when the system is randomly initialized. A similar result is likely to hold for the cases described above. This could only be determined by a full finite-amplitude analysis of the system, which is beyond the scope of this paper.

10. The three-layer system

Results were calculated for a three-layer configuration with an impermeable upper boundary (case *A*) where an aquifer was positioned centrally between two layers of another material, whose permeability is different from that of the middle layer (i.e. $r_3 = r_1$ and $K_3 = K_1$). Again, it was assumed that the layer conductivities were equal (i.e. $k_3 = k_2 = k_1$). Values of $R_{c\min}$, L and σ for the depths $r_1 = 0{\cdot}1$, $0{\cdot}2$, $0{\cdot}3$, $0{\cdot}4$, $0{\cdot}475$ and $0{\cdot}495$ (corresponding to middle-layer thicknesses of $0{\cdot}8$, $0{\cdot}6$, $0{\cdot}4$, $0{\cdot}2$, $0{\cdot}05$ and $0{\cdot}01$) and for the permeability range $10^{-3} \leqslant K_2/K_1 \leqslant 10^3$ are shown in figure 12. (Some results for the particular case $r_1 = 0{\cdot}4$, $L = 1{\cdot}0$ are given in McKibbin & O'Sullivan (1980).)

For the range where the permeability ratio is not extreme, comments similar to those made for the two-layer case apply. For certain layer thicknesses, bifurcation in the graphed values occur at certain permeability ratios. For thick middle layers of fairly small permeability, convection throughout the entire depth of the system implies wide cells, with widths of over twice the total depth, and large values of σ. These correspond to wide areas of heating at the base for each cell, and consequent wide areas for cooling on the upper surface.

Systems where the middle layer is thin are of interest because of the geothermal implications of a small relatively impermeable layer cutting through a permeable matrix. The most important effect seems to be the splitting of the convection pattern into two cells, rotating in the same direction, stacked vertically above and below the impermeable stratum. For $r_2 = 0{\cdot}01$ ($r_1 = 0{\cdot}495$) for example, when $K_2/K_1 = 0{\cdot}001$, the aspect ratio of each cell is approximately $1{\cdot}45$, with $R_c = 2{\cdot}7$ (giving $R_{1c} = R_{3c} = 26{\cdot}1$) and $\sigma = 2{\cdot}15$. The temperature difference required to destabilize this system is thus $2{\cdot}7$ times that required if the impermeable layer was not there. The coefficient σ is not very different from that for a homogeneous layer, however (the value for the latter is $\sigma = 2$). Because the middle layer acts as a linking conductor between the cells, the system is not just behaving like two separate homogeneous-layer problems stacked on top of each other. This is only the case when the middle layer is infinitely conducting and is hence isothermal, giving $R_{1c} = R_{3c} = 4\pi^2$. This corresponds to the homogeneous-layer onset problem where the vertical wavenumber is 2, giving a critical Rayleigh number $R_c = 4$ for $L = 0{\cdot}5$, with two square counter-rotating cells one above the other.

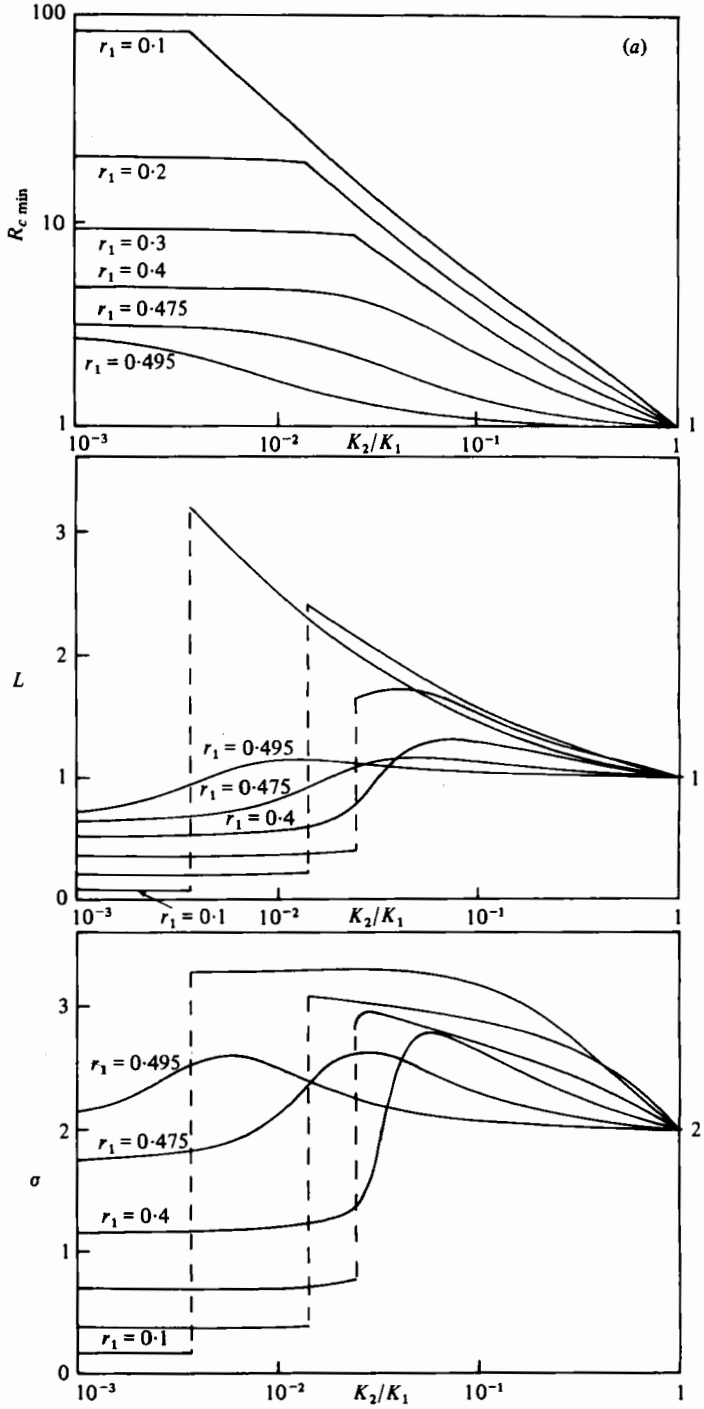

FIGURE 12 (*a*). For legend see p. 169.

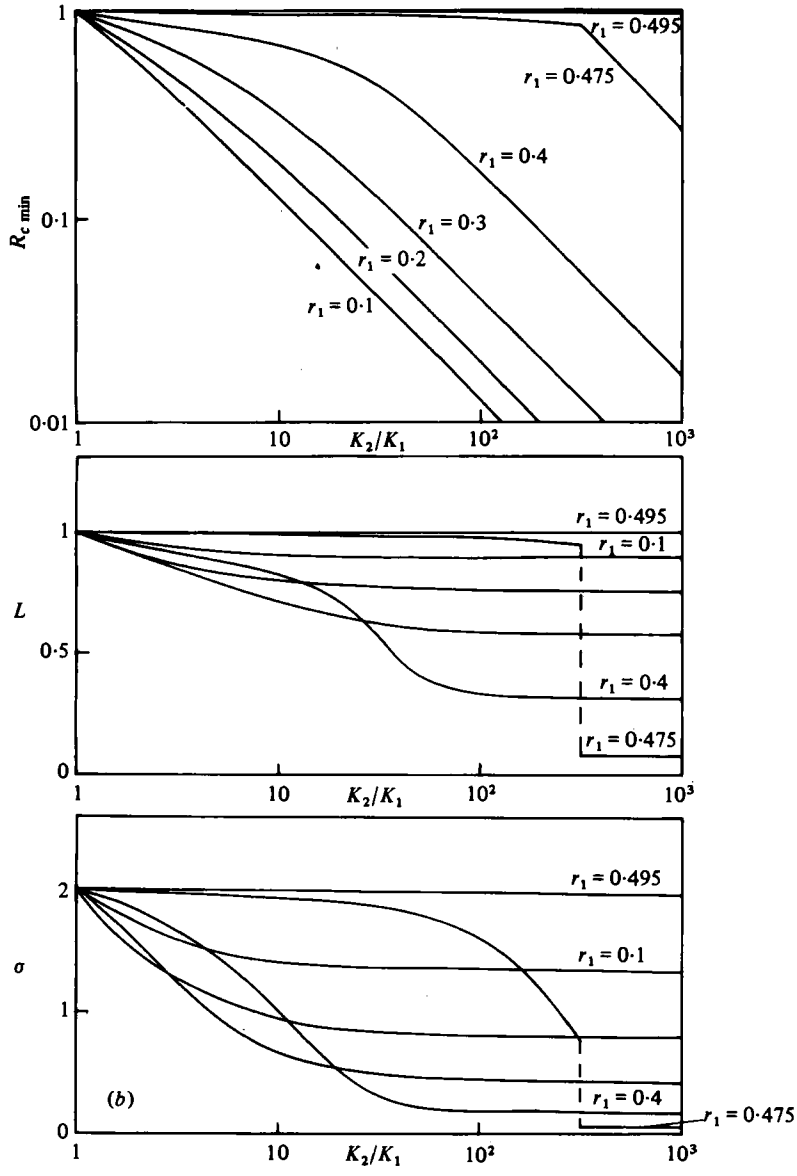

FIGURE 12. Values of $R_{c\min}$, L and σ for an infinite three-layer system with a closed top, with $r_3 = r_1$, $K_3 = K_1$. (*a*) $10^{-3} \leqslant K_2/K_1 \leqslant 1$; (*b*) $1 \leqslant K_2/K_1 \leqslant 10^3$.

The only published results for finite-amplitude convection in a three-layer system are those by Rana *et al.* (1979), who considered a specific configuration modelling the Pahoa reservoir. Three cases were considered, two where the (fixed) sides of the region were heated, and one (case III) where they were insulated. The present study can be applied to the last case. For the depths and permeability ratios given ($r_1 = 0{\cdot}4375$, $r_2 = 0{\cdot}25$, $r_3 = 0{\cdot}3125$, $K_2/K_1 = 0{\cdot}4$, $K_3/K_2 = 6{\cdot}25$) calculation shows that the critical value of R for the system is given when there are two cells in the reservoir. (Instead of minimizing R_c for continuously varying L, it is minimized over

the values of L corresponding to 1, 2, 3, ... cells in the reservoir (which has a width to height ratio of 2).) This value is $R_c = 0{\cdot}838$, giving a value of 33·1 for Ra_1 as defined by Rana *et al.* The value of this parameter for which their results were found is $Ra_1 = 300$, more than 9 times critical. An interesting point is that, even at this high Rayleigh number, two cells appear to remain the preferred pattern in the reservoir. Estimation of the value of Nu in this case using the present analysis is inappropriate because of the high Rayleigh number.

11. Equivalent parameters for a layered system

The difficulties associated with modelling the complex structure of an actual geothermal system leads naturally to simplified models. Observation of average heat flux through the surface of a geothermal region does not in general allow direct deduction of the structure. Assumption of a homogeneous aquifer allows calculation of average permeability and thermal conductivity; however, as is shown below, layering of the system can have marked observable effects on the convective heat flux.

We first define 'equivalent' thermal conductivity and permeability for a general layered system. These quantities are such as to render, for a given average temperature gradient $\Delta T/d$, the inhomogeneous system indistinguishable from a homogeneous layer up to the point of onset of convection.

In a layered system, the heat transferred by conduction alone is

$$\begin{aligned} Nu_c^* &= \frac{1}{l}\int_0^l \left(-k_1 \frac{\partial T_c}{\partial z}\right)_{z=0} dx \\ &= \Delta T/\delta \end{aligned}$$

as given previously in §2; the heat transferred by a homogeneous layer with an 'equivalent' conductivity k_e, is $k_e \Delta T/d$. For these two quantities to be equal requires

$$\frac{k_e}{k_1} = \frac{d}{k_1 \delta} = 1 \Big/ \sum_{i=1}^{N} \frac{r_i}{k_i/k_1}.$$

This gives the equivalent conductivity of the layered porous medium as $k_e = d/\delta$.

An equivalent permeability, K_e, for the layered system can be worked out by considering the minimum value of R at which onset of convection can occur. At onset, the equivalent homogeneous layer has a Rayleigh number R_h, given by

$$\frac{\rho_a g \alpha c \Delta T_c d K_e}{4\pi^2 \nu k_e} = R_h.$$

Similarly, the layered system has a Rayleigh number R_c at onset, given by

$$\frac{\rho_a g \alpha c \Delta T_c d K_1}{4\pi^2 \nu k_1} = R_c.$$

Upon division, we have

$$\frac{K_e}{K_1} = \frac{R_h}{R_c}\frac{k_e}{k_1}.$$

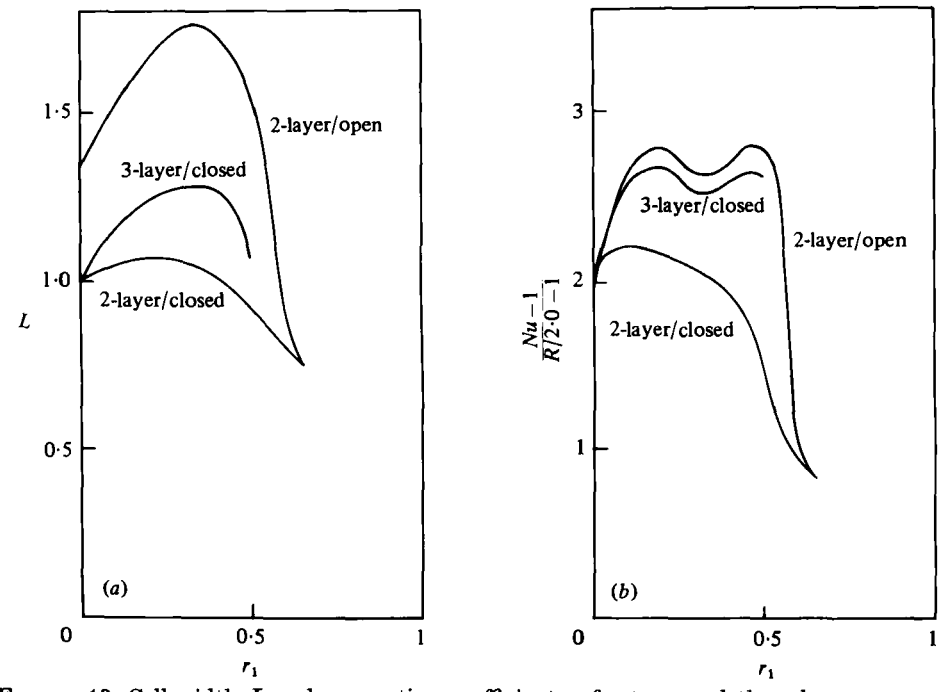

FIGURE 13. Cell-width L and convection coefficient σ for two- and three-layer systems which have equivalent conductivity and permeability, and for which convection may begin for $R_c = 2{\cdot}0$.

Certain combinations of layer depths and relative permeabilities and conductivities of different layered systems will give the same equivalent permeabilities and conductivities. At onset of convection the only distinguishable property will be cell-width which may or may not be observable. However, the expression for the Nusselt number for all the systems has the same form, namely

$$Nu = 1+\sigma\left(\frac{R}{R_c}-1\right) = 1+\sigma\left(\frac{\Delta T}{\Delta T_c}-1\right).$$

Because the values of σ vary widely with different layered configurations, the heat transferred at supercritical Rayleigh numbers may also vary widely, even though the equivalent systems are indistinguishable up to the critical point.

In order to make direct comparisons between systems which are equivalent, we investigate values of L and σ for laterally unbounded configurations which give $R_c = 2{\cdot}0$. This means that onset occurs in each of these systems, assumed to be of the same depth, at the same temperature difference ΔT_c. We choose $k_e/k_1 = k_i/k_1 = 1{\cdot}0$, and it then follows that $K_e/K_1 = 0{\cdot}5$ for the closed-top systems, and $K_e/K_1 = 0{\cdot}343$ for the open-surface cases. Thus, for all these systems, conduction of heat is the same up to the point of onset, which also occurs at exactly the same temperature difference for each configuration. There the similarity ends, however. The cell-width and amount of heat transferred by conduction and convection together differ markedly from model to model, as shown in figure 13. (The two-layer graphs are truncated at $r_1 \simeq 0{\cdot}65$ since for large lower-layer depths there are no equivalent systems, no matter what the value of K_2/K_1. The three-layer graphs similarly are truncated at $r_1 \simeq 0{\cdot}498$.) Figure 13(*b*) gives a direct comparison of the heat transferred by the

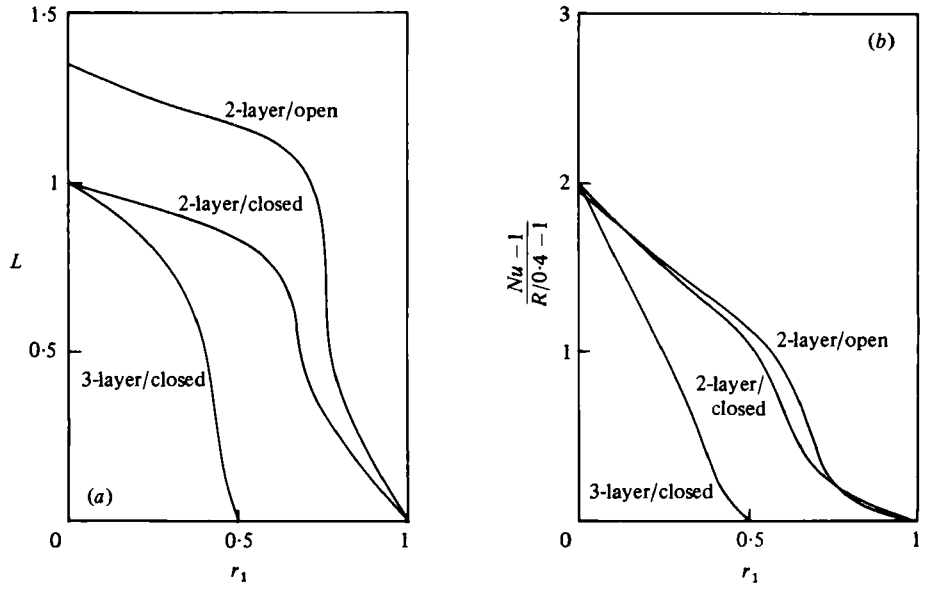

FIGURE 14. Cell-width L and convection coefficient σ for two- and three-layer systems which have equivalent conductivity and permeability, and for which convection may begin for $R_c = 0{\cdot}4$.

'equivalent' systems – the values vary markedly with r_1, and also with whether the system has 2 or 3 layers, or has an open or closed upper surface. At some temperature difference $\Delta T > \Delta T_c$, the two-layer open system is, in most cases ($r_1 > 0{\cdot}05$), the one which transfers most heat, with the three-layer system close to it. The two-layer closed model has narrower cells, and less heat-transport capacity than either of the above, except near $r_1 = 0$ and at $r_1 = 0{\cdot}65$ (the latter value corresponds to the limit $K_2/K_1 \to 0$, when both two-layer systems become effectively the same).

That these comments are not generally applicable to all cases is easily seen in figure 14, where the results for systems corresponding to $R_c = 0{\cdot}4$ are shown. (Again, we chose $k_e/k_1 = k_i/k_1 = 1{\cdot}0$, and then $K_e/K_1 = 2{\cdot}5$ for the closed systems and $K_e/K_1 = 1{\cdot}716$ for those which are open.) Here, the cell-widths and heat transferred are in all cases less than for the homogeneous cases, both sets of values decreasing with increasing r_1. For each value of the lower-layer depth the narrowest cells and smallest heat transfer attach to the three-layer system, while the heat transferred by the two-layer systems are much the same. The most important observation is that these equivalent systems may convect heat at any rate from that corresponding to a homogeneous system, down to zero.

12. Conclusions

The inclusion of more physical realism in the matrix properties of the medium is important for the accurate modelling of the heat transfer characteristics of a porous medium heated from below. This complements the results obtained (see, for example, Straus & Schubert 1977) when more realistic properties of water, such as temperature-dependent viscosity, are included. Cell-width at onset is little affected by water properties. The present work shows that the presence of layers of different per-

meability can have great influence on the convective flow in a porous medium heated from below. Because the slope of the Nusselt number graph varies with cell-width in a layered porous medium the heat transferred through a geothermal system depends considerably on the layering of materials comprising the matrix. This indicates that the modelling of such systems by a homogeneous layer may give quite erroneous predictions as far as convection pattern and heat flux are concerned.

REFERENCES

CALTAGIRONE, J. P. 1975 *J. Fluid Mech.* **72**, 269.

COMBARNOUS, M. A. & BORIES, S. A. 1975 *Adv. Hydrosci.* **10**, 231.

CHENG, P. 1978 *Adv. Heat Transfer* **14**, 1.

ELDER, J. W. 1967 *J. Fluid Mech.* **27**, 29.

HORNE, R. N. & O'SULLIVAN, M. J. 1978*a* *Phys. Fluids* **8**, 1260.

HORNE, R. N. & O'SULLIVAN, M. J. 1978*b* *Trans. A.S.M.E.* C, *J. Heat Transfer* **100**, 448.

JOSEPH, D. D. 1976 *Stability of Fluid Motions*. Springer.

LAPWOOD, E. R. 1948 *Proc. Camb. Phil. Soc.* **44**, 508.

MALKUS, W. V. R. 1954 *Proc. Roy. Soc.* A **225**, 196.

MASUOKA, T., KATSUHARA, T., NAKAZONO, Y. & ISOZAKI, S. 1978 *Heat Transfer: Japan. Res.* **7**, 39.

MCKIBBIN, R. & O'SULLIVAN, M. J. 1980 *J. Fluid Mech.* **96**, 375.

PALM, E., WEBER, J. E. & KVERNVOLD, O. 1972 *J. Fluid Mech.* **54**, 153.

RANA, R., HORNE, R. N. & CHENG, P. 1979 *Trans. A.S.M.E.* C, *J. Heat Transfer* **101**, 411.

SCHUBERT, G. & STRAUS, J. M. 1979 *J. Fluid Mech.* **94**, 25.

STRAUS, J. M. 1974 *J. Fluid Mech.* **64**, 51.

STRAUS, J. M. & SCHUBERT, G. 1977 *J. Geophys. Res.* **82**, 325.

STRAUS, J. M. & SCHUBERT, G. 1978 *J. Fluid Mech.* **87**, 385.

STRAUS, J. M. & SCHUBERT, G. 1979 *J. Fluid Mech.* **91**, 155.